

NATIONAL ADVISORY COMMITTEE FOR AERONAUTICS

TECHNICAL NOTE 2783

USE OF A CONSOLIDATED POROUS MEDIUM FOR MEASUREMENT OF
FLOW RATE AND VISCOSITY OF GASES AT ELEVATED
PRESSURES AND TEMPERATURES

By Martin B. Biles and J. A. Putnam

University of California



Washington
September 1952

TECHNICAL NOTE 2783

USE OF A CONSOLIDATED POROUS MEDIUM FOR MEASUREMENT OF
FLOW RATE AND VISCOSITY OF GASES AT ELEVATED
PRESSURES AND TEMPERATURES

By Martin B. Biles and J. A. Putnam

S U M M A R Y

The use of a consolidated porous medium as a gas-metering device and for determination of gas viscosity has been investigated over a moderate range of temperature and pressure. With normal laboratory techniques it appears possible to calibrate large porous Alundum filtering thimbles to meter gas with a probable error of 0.1 to 0.2 per cent. The geometry of such elements permits an appreciable range of gas flow rate to be metered with small, accurately controlled, pressure drops. The advantages of such a device warrant its use as a laboratory instrument.

Results of the flow tests have been employed in the determination of the viscosity of air up to approximately 900 pounds per square inch absolute at the two test temperatures of 75° and 517° F. These data appear to check sufficiently well with other published viscosity data to justify the use of this method as a recommended procedure.

I N T R O D U C T I O N

The primary objective of this report is to present the results of a laboratory investigation designed to determine the factors involved in the employment of porous mediums as laboratory metering devices for gas flow. Preliminary inspection and analysis of the laws governing gas flow through such substances suggest that they would serve ideally in this capacity. The linearity of the flow characteristics, as specified by Darcy's law, should prove to be an especially attractive advantage in control of the flow.

A second application of the results of the porous flow tests is the determination of the viscosity of gases at high temperatures and pressures. In this latter analysis the recent hypothesis of Klinkenberg (reference 1) suggests a method of conveniently determining these data.

This investigation was conducted at the University of California under the sponsorship and with the financial assistance of the National Advisory Committee for Aeronautics.

SYMBOLS

A	gross cross-sectional area of flow, square feet
b	constant ($4\mu P_m/\epsilon R$)
D_e	effective pore diameter of porous medium, feet
f	Fanning friction factor, dimensionless
g	acceleration due to gravity, feet per second
K	permeability of porous material, darcys or millidarcys
K_a	apparent permeability of porous material, darcys or millidarcys
K_{liq}	permeability of porous material to liquids, darcys or millidarcys
L	thickness of porous material or distance in direction of flow, feet
m	porosity of porous material, void volume divided by bulk volume
P	absolute pressure, pounds per square inch absolute
P_m	arithmetic mean of pressures P_1 and P_2 , pounds per square inch absolute
P_1	absolute pressure at entrance to capillaries
P_2	absolute pressure at exit from capillaries
ΔP	pressure differential across capillaries, pounds per square inch
q	volumetric flow rate per unit gross cross-sectional area (Q/A)
Q	volumetric flow rate, cubic feet per second

Q_m	volumetric flow rate corrected to mean temperature and pressure conditions, cubic feet per second
R	radius of capillaries, feet
T	temperature, $^{\circ}\text{K}$
T_m	mean air temperature, $^{\circ}\text{F}$
V	velocity of flow through capillaries, feet per second (Q/mA)
V_m	velocity of flow through capillaries corrected to mean temperature and pressure conditions
W	specific weight of fluid flowing, pounds per cubic foot
W_m	specific weight of fluid flowing corrected to mean temperature and pressure conditions
X	distance measured in direction of flow, feet
μ	absolute viscosity of fluid flowing, pound seconds per square foot
ϵ	coefficient of friction of gas, a constant of walls and of gas, dimensionless
ρ	mass density of fluid flowing, slugs per cubic foot
$\rho_0 = P/RT$	

F L O W O F F L U I D S T H R O U G H

A P O R O U S M E D I U M

DARCY'S LAW

The granular materials in a porous medium form a solid framework within which the voids form the fluid passages. These passages vary in size and shape and are interconnected. Accordingly, the problem becomes one of nonuniform flow. Theoretically, the problem is covered by the classical hydrodynamics, at least in the viscous flow regime. However, the formal solution of the basic equations is a hopeless task owing to the intricate geometrical boundaries of the multiple connected maze of capillary channels. By considering the porous aggregate macroscopically as a continuous medium for fluid transmission, the detailed

structure with its tremendous internal surface area can be averaged out and replaced dynamically by an equivalent continuous and uniform medium with a fluid-transmission coefficient, or permeability K , as defined by equation (1).

The quantitative theory of the flow of homogeneous fluids through porous mediums was initially developed by Darcy in 1856 (see reference 2). In a series of classical experiments Darcy studied the flow of water through sand filters and found that the volumetric rate of flow through a porous body is directly proportional to the cross-sectional area of flow and the head loss across the faces of the body and inversely proportional to the thickness of the medium and the absolute viscosity of the fluid, provided the nature of the flow is laminar. This empirical law can be expressed analytically in the form

$$q = -\frac{KW}{\mu} \frac{d}{dL} \left(\frac{P}{W} + z \right) \quad (1)$$

where

q volume flux per unit gross area of medium (Q/A)

Q total volume rate of flow

A gross area of cross section normal to flow

W specific weight of fluid

μ absolute viscosity of fluid

$\frac{d}{dL} \left(\frac{P}{W} + z \right)$ gradient of hydraulic potential or head at point where q is determined (negative sign denotes decreasing potential in direction of flow)

L distance in direction of flow

P absolute pressure

z elevation in gravitational field

K permeability of medium

The effective flow boundaries of the system are those which define the extent of the porous medium rather than the myriad internal particle

surfaces. The structure of the medium is characterized by the permeability K . In principle, it is to be considered as a function only of the space coordinates and is locally independent of the nature of the fluid so long as the latter is in a single phase. The viscosity μ is the only property of the fluid which is dynamically significant.

The standard unit of permeability of a porous medium to fluids is the "darcy," which is defined as the rate of flow in milliliters per second of a fluid of 1 centipoise viscosity through a cross section of 1 square centimeter of a porous medium under a pressure gradient of 1 atmosphere (76.0 cm of mercury) per centimeter and conditions of viscous flow. For convenience, a subunit, the millidarcy, equaling 0.001 darcy, is often used. As can be seen from equation (1), the permeability constant K has the dimensions of length squared. Accordingly, the following conversion factors will be useful:

$$\text{Darcys} \times 1.062 \times 10^{-11} = \text{Square feet}$$

$$\text{Darcys} \times 9.86 \times 10^{-9} = \text{Square centimeters}$$

PERMEABILITY OF POROUS MEDIUM TO LIQUIDS AND GASES

For liquids flowing horizontally through a porous bed, in the absence of a free surface, equation (1) may be written in the following integrated form

$$Q = \frac{KA}{\mu} \frac{\Delta P}{L} \quad (2)$$

where ΔP is the difference in pressure between two parallel faces normal to the direction of flow and where L is the distance between these faces.

For gas flow the variation of specific weight with pressure must be taken into account in integrating equation (1). For pressure changes which permit use of the perfect gas law equation (1) becomes for isothermal flow

$$Q_m = \frac{KA}{\mu} \frac{\Delta P}{L} \quad (3)$$

where Q_m is the total volume rate of flow evaluated at the arithmetic mean pressure existing in the medium.

Permeability of Porous Medium to Liquids

Numerous investigators have presented experimental evidence substantiating the belief that a permeable substance retains consistent flow characteristics with different liquids (references 1 to 3). Klinkenberg made extensive tests with nine different organic liquids and water on several cores of varying permeabilities and showed that the permeability was essentially independent of the nature of the liquid (reference 1). Calhoun and Yuster presented similar data on the flow of water and organic and inorganic liquids through various glass and silica beds and arrived at the same conclusion (reference 3). These latter authors extended their investigations to the measurement of liquid permeability over a range of temperatures from 0° to 60° C for several liquids. The results of these tests show that there is no variation in liquid permeability with temperature. Grunberg and Nissan had previously reported that liquid permeability should decrease with a decrease in temperature (reference 4). In behalf of their conclusions, Calhoun and Yuster argued that if any variation with temperature is to be expected, it should be in the direction of an increase in permeability with temperature. This reasoning was based on the probable effect of thermal-expansion characteristics on the size of the interstices. Inasmuch as their cores were manufactured from silica and glass, substances with very low thermal coefficients of expansion, it might be anticipated that the effect of temperature variations on permeability would be very small.

Permeability of Porous Medium to Gases

Until recent years it had been generally assumed that the permeability of a substance was constant regardless of the phase of the fluid passing through it. On this assumption it was common practice to determine the permeability of a core with air and apply the results when other gases or liquids were passed through the same core. As a result of his investigations in 1941, Klinkenberg showed that (1) the permeability of a porous body to liquids and gases will be different, (2) the permeability will be different for different gases, unless the gases have the same molecular concentration, and (3) the permeability to gases will depend on the mean pressure of flow. These effects were attributed to the mean free path of the gas molecules, indicating that the permeability of a porous substance to a gas must be a function of the pressure, temperature, and nature of the gas.

Theory of slip.- By reference to the kinetic theory of gases it can be shown that the law of Poiseuille holds until the mean free path of the molecules approaches the dimensions of the tube through which the gas is flowing. This will occur when the pressure of the gas is greatly reduced or the dimensions of the tube assume minute proportions. Under

these conditions the failure of Poiseuille's law results from the velocity at the wall being greater than zero; that is, the gas seems to slip past the wall. The amount of gas flowing through a tube would then appear to be greater than the diameter of the tube would permit. The phenomenon of slip in a capillary tube can be taken under consideration by applying a correction to the usual equation of flow. Thus

$$V = \frac{(P_1 - P_2)}{8\mu L} R^2 \left(1 + \frac{4\mu}{\epsilon R} \right) \quad (4)$$

If R is large compared with $4\mu/\epsilon R$ the correction term can be neglected and the equation reverts to that of Poiseuille. The ratio μ/ϵ is commonly referred to as the "coefficient of slip" and is proportional to the mean free path of the gas molecules.

Klinkenberg effect.- Klinkenberg visualized the flow through a porous substance as that in which all the capillaries in the material are of the same diameter and are oriented at random throughout the solid substance. The theory of slip can be applied to such an idealized model to make possible certain qualitative predictions. It has previously been mentioned that the slip correction is proportional to the mean free path; it can further be stated that the mean free path is inversely proportional to the pressure. Then $4\mu/\epsilon R = b/P_m$, where b is a constant. Klinkenberg applied this result to the flow through the multiple capillaries of a porous body and rewrote equation (3) in the form

$$Q_m = \frac{KA(P_1 - P_2)}{\mu L} \left(1 + \frac{b}{P_m} \right) \quad (5)$$

where $P_m = (P_1 + P_2)/2$, and the other symbols are as listed. It becomes obvious that the apparent permeability of a porous medium to a gas can be represented by

$$K_a = K_{liq} \left(1 + \frac{b}{P_m} \right) \quad (6)$$

where K_{liq} is intended to represent the "true permeability" of the substance, or its permeability to liquids.

From equations (5) and (6) several important aspects are deducible. Referring to figures 1 and 2 it is seen that gas permeability is a linear function of the reciprocal mean pressure of the flow. If the curve for the apparent permeability K_a is then extrapolated to infinite mean pressure, the slip-correction factor assumes unit value and the extrapolation should give the true permeability, as shown by K_{liq} . As the constant b (where $b = 4\mu P_m / \epsilon R$) is inversely proportional to the radius of the capillaries, its value might be expected to be small for mediums of high permeability and large for mediums of low permeability. This response produces the effect shown in figure 1 on the slope of the K_a curve for tight and loose cores. Figure 2 illustrates the influence of the mean free path of the gas on the value of K_a . When the mean free path is large, b will be correspondingly large and the curve for K_a will be steep. It is crucial to realize that at the same temperature the K_a curve for all gases passing through a particular core will extrapolate to give K_{liq} . In any event the gas permeability does not depend on pressure difference, so long as the mean pressure is constant, and viscous flow obtains.

RANGE OF VALIDITY OF DARCY'S LAW

For purposes of demonstrating the effects of a continued increase in the pressure drop across a porous body on the linearity of Darcy's law, it is preferable to write equation (3) in the form

$$\frac{K}{\mu} = \frac{Q_m/A}{\Delta P/L} \quad (3a)$$

If a plot is made of Q_m/A against $\Delta P/L$ up to very large pressure differentials a curve similar to that shown in figure 3 will result. The equation for flow through a porous medium is valid only as long as the resulting plot of Q_m/A against $\Delta P/L$ is linear and intersects the origin. Above a certain limiting pressure drop the curve becomes nonlinear and assumes a concave appearance toward the $\Delta P/L$ -axis. This produces a lower flow rate than that predicted from Darcy's law and indicates that energy is being dissipated at an increased rate within the capillaries, resulting in the nonlinear velocity-pressure-drop relationship.

If the same quantities, Q_m/A against $\Delta P/L$, are plotted on logarithmic coordinates a configuration such as that illustrated in figure 4 results. This form of plotting can be employed advantageously to illustrate the various regimes of flow that can exist in porous structures. At low pressure differentials the nature of the flow is viscous and is characterized on this plot by a straight line having a slope of 45° . When the pressure differential is increased beyond the limits of the viscous regime, the inertia forces caused the flow to separate from microscopically diverging boundaries with subsequent formation of eddies which consume energy at a higher rate than does strictly laminar motion and the curve will fall away toward the $\Delta P/L$ -axis. As these eddies develop in all the capillaries the curve again appears as a straight line, but now at a slope of 26.5° with the horizontal. Limited experiments indicate that, with a further increase in the pressure differential, compressibility effects may become important and the curve will again bend toward the abscissa. The behavior in this region may be characterized by the gradual formation of shock waves in the capillaries so that, at sufficiently high pressure drops, the curve might be expected to become parallel to the $\Delta P/L$ -axis. The three portions of the curve will be separated by definite transition regions, since inconsistencies in the shapes and sizes of the capillaries will prevent sharp transitions.

EXTENSION OF FANNING EQUATION TO FLOW THROUGH A POROUS MEDIUM

The Fanning equation, which is frequently used to compute the head loss due to steady fluid flow in straight pipes of circular cross section, can be applied to the flow through a porous medium when written in the form:

$$\frac{dP}{dX} = 2f \frac{WV^2}{gD_e} \quad (7)$$

where f is the Fanning friction factor, a function of the Reynolds number, and D_e is the effective pore diameter of the porous medium and may be defined as the diameter of a single uniform capillary which will discharge the same amount of fluid per unit time under the same pressure gradient as in the porous medium. Noting that $W = W_m P/P_m$, $W = W_m Q_m/Q$, and $V = Q/mA$, where the subscript m again refers to the mean flow conditions and the symbol m is the porosity of the medium

through which flow occurs, equation (7) may be integrated to give the result

$$f = \frac{gD_e m^2 (\Delta P/L)}{2W_m (Q_m/A)^2} \quad (8)$$

The Reynolds number for the flow of a fluid through a porous body can be expressed in the form

$$\frac{V_m D_e \rho}{\mu} = \frac{D_e W_m (Q_m/A)}{gm\mu} \quad (9)$$

To make a correlation between equations (8) and (9) possible, an expression must be derived for the effective pore size D_e . This can be readily accomplished by resorting to the law of Poiseuille,

$$\frac{dP}{dX} = \frac{-32\mu V}{D_e^2} \quad (10)$$

where the symbols are as previously defined. Noting that

$$V = \frac{Q}{mA} = \frac{Q_m P_m}{mA P} \quad (11)$$

and substituting equation (11) into equation (10),

$$\int_{P_1}^{P_2} P \, dP = -\frac{32\mu Q_m P_m}{mA D_e^2} \int_0^L dX \quad (12)$$

The result of this integration is

$$\frac{\Delta P}{L} = \frac{32\mu Q_m}{mA D_e^2} \quad (13)$$

It may be recalled that Darcy's law can be written

$$\frac{\Delta P}{L} = \frac{\mu Q_m}{KA} \quad (14)$$

In view of the definition of the equivalent pore diameter D_e , equations (13) and (14) may be equated, resulting in

$$D_e = \sqrt{32K/m} \quad (15)$$

If D_e is to assume the dimensions of a length, K must be expressed as the square of a length. Inasmuch as 1 darcy = 1.062×10^{-11} square foot, the equation for D_e may be written

$$D_e = 1.843 \times 10^{-5} \sqrt{K/m} \quad (16)$$

The limit of validity of Darcy's law can be further demonstrated by plotting values of the friction factor from equation (8) against the Reynolds number as computed from equation (9). When this is done a plot such as that shown in figure 5 results. As demonstrated above when the Reynolds number is below 0.2 experimental results agree with the curve for viscous flow in circular pipes. Above a Reynolds number of 0.2 the results tend to diverge from the Fanning curve, indicating increased energy losses. This correlation indicates the limit of validity of Darcy's law to be at a Reynolds number of approximately 0.2, when computed as indicated by equation (9). Below this value the flow will be independent of the permeability.

LABORATORY EXPERIMENTATION

DESCRIPTION OF APPARATUS

General Description

Schematic flow diagrams, photographs, and sectional drawings of the equipment employed during the investigation are shown in figures 6 to 11.

Prominent components of the system were the compressor, metering unit, manometer, and test meter. Less prominent equipment included the necessary tubing, valves, receiver, pressure regulators, heating and cooling coils, an air-humidifying apparatus used in conjunction with the test meter, and a cathetometer to determine manometer differentials.

Gas Supply

Air under pressure was supplied by a 5-horsepower, two-stage compressor capable of delivering approximately 10 cubic feet per minute of free air at a pressure of 1000 pounds per square inch gage. The gas was passed through a water-cooled coil for the purpose of condensing a portion of the accompanying water vapor and thence into a receiver of approximately 0.75-cubic foot capacity. The receiver was equipped with a drain for continuous removal of the accumulated moisture. This arrangement provided a supply of air containing a moisture content of 0.0002 and 0.00016 part by weight at receiver pressures of 800 and 1000 pounds per square inch gage, respectively. All tests were made with the receiver pressure maintained within these limits.

Control of the gas pressure in the metering unit was accomplished by two of the highest-quality pressure regulators. One regulator was employed for meter pressures in the range of 0 to 300 pounds per square inch gage; the second regulator controlled meter pressures above 300 pounds per square inch gage. It was found that these regulators sustained sufficiently stable downstream pressure conditions provided the receiver pressure exceeded the desired metering pressure by 300 pounds per square inch gage. When such a differential could not be maintained because of limitations of the compressor, it was necessary to hold the receiver pressure constant. This was effected by allowing the compressor to operate continuously during the test and bleeding off the surplus air.

Test-Gas Heating

Provisions for heating of the test gas to high temperatures were provided by gas and electrical heating elements. The gas-heating unit consisted of twenty 3-inch-diameter coils of heavy-wall Monel-metal tubing heated by a large gas burner. Close-fitting guides directed the hot gases of combustion over the coils. The burner was equipped for forced primary air supply.

To provide for more accurate control of the test-gas temperature than could be accomplished by use of the gas heater alone, a 24-inch length of stainless-steel tubing connecting the heater to the adjacent metering unit was wrapped with insulated Nichrome resistance tape. By

means of this electrical heating element an additional 700 watts of energy could be supplied the test gas. Close control of the electrical power was provided by a "stove" type step resistor in conjunction with a slide wire resistor. The use of both means of heating simultaneously could heat the test gas to over 1000° F.

Metering Unit

The metering unit (fig. 6) was designed to withstand simultaneous pressure and temperature conditions of 2000 pounds per square inch and 1000° F, respectively. All components were constructed of Inconel metal to gain the advantages of high-temperature strength characteristics and uniformity of thermal expansion. Incoming gas was passed immediately through a filtering and drying assembly. This assembly consisted of approximately 1 pound of silica gel desiccant packed between two Alundum disks of 3/16-inch thickness and 1000-millidarcy permeability and supported within an appropriate container. This container was installed in the metering unit by means of internal threads within the metering case. Such an arrangement was intended to place the filtering and drying assembly a minimum distance ahead of the metering element, with no intermediate external connections or joints. Periodic inspection of the desiccant indicated that the drying agent was not necessary if the receiver pressure exceeded 800 pounds per square inch gage. The desiccant was retained in place throughout the period of the tests because of its value in removing moisture collecting in the system when not operating.

The metering element, across which the measurable gas pressure drop was established, consisted of a large Alundum filtering thimble. The use of such thimbles for this purpose offered several advantages. Their geometry provided a large flow area, small thickness, and good strength characteristics to withstand the pressure differentials. Alundum is known to be extremely stable up to high temperatures, thus permitting a single element to be utilized over a wide temperature range.

Four thimbles with approximate permeabilities of 200, 60, 15, and 5 millidarcys were manufactured specially for this investigation by the Norton Co. from the highest-purity Alundum. Preliminary computations indicated that this group of thimbles would give satisfactory pressure differentials with atmospheric flow rates in the range 0.2 cubic foot per minute to 75 cubic feet per minute. No adhesives were used to bind the particles of these thimbles, the bonding being accomplished by firing the material to approximately 3000° F. Because of this method of manufacture it was not possible to maintain uniformity of diameter or wall thickness of the thimbles. The finished products were 12.5 inches long, varied in diameter from 2.5 to 2.9 inches, and varied in wall thickness from 1/4 to 3/8 inch. The flow areas ranged from 85 to

90 square inches in the four thimbles. The porosity of the Alundum was approximately 26 percent.

Prior to utilization of these porous thimbles as flow-meter elements it was necessary to provide a gastight seal and means of mounting at the open end of the tube. The following procedure was found to satisfy these requirements most conveniently: The open face and adjacent 1/2 inch of the thimble surface were coated with brass by a metal-spraying process. Excellent adhesion of the sprayed metal to the Alundum was attained if the latter was preheated to above 500° F. A 0.010-inch-thick copper sleeve was slipped over the coated end of the thimble and silver-soldered to the sprayed metal. Thermal stresses were relieved by performing this operation with the assembly at approximately 1000° F. The opposite end of the copper sleeve was then fastened similarly to an appropriate flange. Finally, a perforated steel supporting basket was slipped inside the thimble and welded to the flange. The sole purpose of this basket was support of the heavy thimble when the copper sleeve softened under elevated temperatures.

It is to be noted that the pressure differential across the thimble was such that the gas flowed radially inward through the cylindrical shell. This was intended as a safeguard against rupturing the Alundum, since the thimbles are undoubtedly capable of withstanding a greater pressure differential if applied to the outside. Photographs of unmounted and mounted thimbles appear in figures 7 and 8.

Combination thermocouple lead seals and pressure connections were manufactured as illustrated in figure 9 and installed upstream and downstream of the meter element. Sealing of the thermocouple leads against the pressure within the meter case was accomplished by passing the wires separately through soapstone glands and crushing these glands about the wires. At the higher pressures these seals leaked a minute quantity of gas, probably because of the porosity of the powdered soapstone. The quantity of gas thus escaping was considered negligible.

The exterior of the meter case was wrapped with three similar Nichrome resistance strip heaters. Each such heating element was approximately 15 feet in length and could supply up to 1000 watts of energy to the meter case. Control of the power to these heaters was accomplished by a Variac voltage regulator. These heaters proved extremely valuable in bringing the bulky meter case up to operating temperature and maintaining thermal equilibrium during the tests. The meter case was covered with 2 inches of magnesian pipe insulation installed on top of the resistance heaters.

Manometer

For purposes of determining the pressure drop across the metering elements a differential manometer was preferred over other types of instruments because of the known reliability of such devices and the relief from performing exacting calibration tests. A high-pressure differential manometer was designed and constructed as shown in figure 10. The outstanding feature of this instrument is that the high-pressure gas is contained by heavy glass plates, with only the relatively small pressure differential across the meter acting upon the glass tubes containing the manometer fluid. A brief description follows.

All major metal components of the manometer were manufactured from superior-grade stainless steel. The main body of the unit was constructed from a solid block of metal of dimensions $24\frac{1}{2}$ by 7 by 2 inches. Two 20-inch grooves were milled in the wide face of this block to accommodate the straight glass tubes. One groove, that of the low-pressure leg, was equipped with rubber "O" ring-type seals at each end to seal the tube from the body. The high-pressure leg was provided with such a seal only at the lower end of the tube, the upper end of the tube terminating unsealed within the groove. At the lower end of the block a drilled hole, located below the seals, connected the two legs, completing the customary "U" of differential manometer legs. A second internal passage connected the two grooves at a point intermediate between the seals. This arrangement permitted the low-pressure gas to act on the fluid in the sealed leg and the high-pressure gas to act on the fluid in the unsealed leg, as well as on the outside of each tube. It is apparent that this instrument is similar in design to the usual open-leg piezometer with the external pressure on the tubes maintained equal to that upstream of the metering section. The only pressure differential across the tubes, or the tube seals, was that across the meter element, a maximum of 20 inches of mercury.

The external pressure on the tubes was contained by two 1-inch-thick tempered glass plates to permit vision of the tubes. Sealing between the glass plates and the metal body was accomplished by use of large rubber "O" ring seals. An appropriate cover supported the glass plates in location. Accurate spacers were provided to prevent the glass from contacting the metal body and to provide the rubber seals with the specified amount of initial compression. This manometer is considered suitable for pressures to 3000 pounds per square inch gage, which is the recommended pressure limitation for the rubber seals.

Manometer differentials were determined with a Wild (Swiss) cathetometer accurate to 0.001 centimeter. Some difficulty was encountered early in the test program in viewing the mercury menisci because of

the recessed position of the glass tubes. Extreme care was necessary in lighting the liquid columns because of the possibility of creating shadows on the meniscus which would result in erroneous readings. This difficulty was eliminated most satisfactorily by playing a spotlight on each column from the approximate elevation of the column, thus illuminating the crest of the meniscus. Any attempts made to direct a light downward on the columns resulted in reflections from the menisci which prevented viewing them through the telescope.

The mercury for use in the differential manometer was of the highest quality obtainable. Before using any of this mercury in the manometer it was further cleansed by stirring in a quantity of acetone. The fluid to be used was then drained from the bottom by means of a pipette. Considerable foreign matter was removed from the mercury by this operation.

Pressure Determination

The pressure upstream from the metering element was determined by means of standard dead-weight gages. In order to obtain greater accuracy of measurement over the range of pressures encountered in these tests, two dead-weight gages of different scale ratios were employed. One gage, with a 5:1 ratio and a recommended range of 0 to 500 pounds per square inch absolute, was utilized for pressure determinations of 500 pounds per square inch absolute or less. A second gage, with a 40:1 ratio and a recommended range of 0 to 1500 pounds per square inch absolute was utilized for pressures above 500 pounds per square inch absolute. These gages indicated the static pressure acting on the upstream leg of the manometer.

For determination of meter flow pressures below the useful range of the dead-weight gages (20 lb/sq in. gage) a standard open-leg mercury manometer was installed to indicate the downstream meter pressure.

Flow-Rate Measurement

Volumetric flow rates at atmospheric pressure were determined either by utilization of a large wet test meter or a volumetric displacement tank. The wet test meter was manufactured by the American Meter Co., Inc., and appeared satisfactory for use with atmospheric gas flow in the range 0.5 cubic foot to 6 cubic feet per minute. This instrument was calibrated over this range by means of the volumetric tank mentioned above.

A second method of flow-rate determination was that of employing directly the volumetric displacement tank. This apparatus was manufactured for the specific purpose of calibrating volumetric flow meters.

It consisted of a 5-cubic-foot copper drum, open at the bottom, which could be raised or lowered by the gas pressure acting on the inside of the tank. Leakage of the gas from beneath the drum was prevented by an annular water seal, into which the open end of the cylinder submerged when being lowered. An eccentrically mounted counterweight corrected for the displacement of the cylinder, allowing a constant internal gas pressure to produce a constant rate of ascent, regardless of position. A counterweight platform was provided to permit control of the internal gas pressure by imposing an external lifting force on the drum. An open-leg manometer was installed to indicate the internal gas pressure.

Prior to passing the dry air from the meter unit into either the wet test meter or the volumetric tank the gas was bubbled through water in a series of containers. This procedure was followed primarily to humidify the air and prevent any water in the wet test meter from evaporating, causing a change in the calibration. It also served the purpose of simplifying the calculations for volumetric flow rate, since the air could be considered completely saturated subsequent to this bubbling process.

Piping and Valves

All tubing was of 3/8-inch nominal size. Where high temperatures were encountered, stainless-steel tubing and fittings were employed. For all other conditions, heavy-walled copper tubing was installed. Steel needle valves were installed adjacent to each regulator and downstream from the metering unit. This latter valve served to control the flow rate through the meter and to throttle the gas to atmospheric pressure for passage through the metering devices.

Experimental Procedure

The laboratory test procedure was devised with intentions of achieving flow-rate determinations of an accuracy between 1 and 2 parts in 1000. Extreme care was taken to assure that all data were taken under comparable conditions and at established equilibrium. The identical preparation for each test was meticulously followed.

Preparation of Metering Elements

Prior to installation of the mounted thimbles in the meter unit a standard cleaning and drying technique was employed. One gallon of clean carbon tetrachloride was forced (under a pressure of 15 to 20 lb/sq in. gage) through the Alundum element for purposes of cleaning. If the fluid discharged from the interstices was in a discolored condition the washing procedure was repeated. The amount of contamination

of the Alundum appeared insignificant. It is believed that the small amount of contamination that was present probably originated during installation of the flanges and was easily removed by the above cleaning process. Subsequent to the washing procedure the elements were dried in an oven at a temperature of 400° F for a minimum of 5 hours. Upon removal from the oven they were immediately installed in the meter unit in this warmed condition to forestall any absorption of moisture by the Alundum.

Air at a temperature above 500° F was passed through the system at periodic intervals as an added precaution against the accumulation of any contaminating liquids within the meter unit.

Preparation of System for Low-Temperature Tests

Prior to recording any low-temperature test data the receiver pressure was established at 800 to 1000 pounds per square inch gage and a minimum of 100 cubic feet of test gas passed through the system. This procedure was necessary to establish thermal equilibrium within the meter unit and to "run in" the wet test meter. It was found that this instrument would not produce consistent data immediately following a period of idleness. During this preparation period, and during the subsequent tests, the air passing into the receiver was maintained at a maximum temperature of 60° F to insure satisfactory condensation of the accompanying water vapor.

Test Procedure, Low-Temperature Tests

The low-pressure tests were made at meter pressures in the range 16 to 850 pounds per square inch absolute and at flow temperatures in the range 71° to 80° F. No attempt was made to control the temperatures. All atmospheric flow data recorded during these tests were obtained using the wet test meter, although the volumetric displacement tank was occasionally used for check purposes.

At flow pressures below 35 pounds per square inch absolute the downstream meter pressure was determined by use of the open-leg manometer. These tests consisted of single runs only. No attempt was made to establish a definite mean metering pressure, since at these low pressures it was extremely difficult to adjust the two manometers simultaneously to establish a predetermined meter pressure.

At metering pressures greater than 35 pounds per square inch absolute a different laboratory procedure from that used for the lower-pressure tests was followed. In this case the upstream pressure was determined by one of the two dead-weight gages installed for this purpose. Predetermined

meter pressures were maintained by adding fractional weights to the dead-weight gages to correct for the differential pressure across the metering element. At each predetermined pressure a group of test runs was made at varying flow rates within the range of the wet test meter. These results were then averaged to obtain the flow characteristics for the particular mean metering pressure.

A normal test run consisted of passing 4 to 20 cubic feet of air through the system. During the period required for the flow measurement continuous readings were taken of upstream and downstream temperatures, pressures, and pressure differentials. Any variation in these values during the course of the run, or any variation in the temperatures for several minutes thereafter, was cause for repetition of the run. This latter precaution was considered necessary because of the probable lag of the thermocouples in indicating unsteady thermal conditions within the meter case.

Preparation of System for High-Temperature Tests

All flow-rate measurements for the high-temperature tests were made utilizing the volumetric displacement tank described in the section entitled "Laboratory Equipment." The use of this instrument was necessitated by the low atmospheric flow rates encountered during the high-temperature runs. This procedure precluded any preliminary "run-in" period as was required when the wet test meter was operated.

The heating facilities installed for warming the meter case and the test gas made the maintenance of thermal equilibrium difficult unless special precautions were taken. As long as 24 hours of operation was at times required to attain equilibrium conditions, and this equilibrium could be quickly upset by changes in the flow rate because of the considerable heat capacity of the gas heater unit. To circumvent partially these difficulties the following procedure was devised to prepare the system for operation: With no gas flowing, sufficient power was supplied to the meter-case electrical heaters to maintain exactly the desired temperatures within. When this power requirement was established it was continually supplied to the heaters thereafter. The gas flow was then started, utilizing only the electrical test gas heater. With this procedure equilibrium could be effected within several hours following initial gas flow and could be conveniently maintained provided the weight rate of gas flow was not substantially altered. No data were recorded unless thermal equilibrium obtained for a minimum of 1 hour. This eliminated the possibility of a pseudo-equilibrium condition existing as a result of a temporary equality of otherwise fluctuating temperatures.

Test Procedure, High-Temperature Tests

The procedure employed during the low-temperature tests was essentially followed during the high-temperature tests, except as noted below. An open-leg manometer was again installed for determination of the metering pressures when below 35 pounds per square inch absolute. Dead-weight gages were used when operating at higher pressures.

No attempt was made during the high-temperature tests to make a series of runs with varying flow rates at a constant predetermined meter pressure. Such a procedure was not expedient for the high-temperature runs because of the probability of destroying the established thermal equilibrium. All runs were made at substantially the same weight rate of flow for which the system was brought to equilibrium. Precautions were observed to insure that the temperatures remained constant during the test and for several minutes following.

D I S C U S S I O N O F R E S U L T S

COMPUTATION PROCEDURES

The computations leading to the final results were accomplished with the maximum degree of accuracy by means of computing machines. In general the calculations were extended to the decimal place commensurate with the accuracy of the observed data. This procedure produced fifth-place results for the pressure differentials and fourth-place results for atmospheric flow rates, which comprise the most crucial data recorded during the tests. Pressure and temperature data were recorded to fourth-place accuracy.

The most important factor in the computations was the conversion of the measured atmospheric gas flow rates to the corresponding flow rates at mean metering conditions. This conversion required extensive and accurate pressure-volume-temperature data for air. Such data are available only in limited form in the literature or can be obtained through considerable computing effort from such corrected equations of state as those of Beattie-Bridgeman, Wohl, or Keyes.

Satisfactory pressure-volume-temperature data as required were obtained from two sources. Those presented in table 1 (taken from reference 5) were computed from the enthalpy-pressure derivative for air and from experimental compressibility data. Those presented in figure 12 were published in graphical form by Crown (reference 6) and computed from the Beattie-Bridgeman equation. A comparison of values from these two sources for the volume of air at 70° F and from 25 to

1000 pounds per square inch absolute resulted in a maximum deviation of only 0.065 percent. The usually reliable Beattie-Bridgeman equation is generally conceded an accuracy of 0.1 percent, indicating that these two sources provide data that are probably within the accuracy of all experimental measurements, except those of manometer differential obtained through use of the cathetometer. Where the data of reference 5 were employed to compute values of Q_m , the value of the volume, as given in table 1, that most closely corresponded to actual test conditions was selected and then corrected to these conditions by use of the perfect gas law.

For purposes of computing atmospheric flow rates the air passing through the humidifier into either the wet test meter or the volumetric displacement tank was considered saturated at the temperature existing within the particular flow-rate instrument employed.

The differential manometer readings were corrected for the density of the air above the mercury columns at all pressures. Density values for mercury were obtained from compressibility data published in the International Critical Tables (reference 7). Density values for air were computed from the data presented in table 1. Table 2 shows the density of mercury corrected for the density of air at the manometer conditions encountered during the tests.

Substantiated values for the viscosity of air at atmospheric pressure, required for the solution of Darcy's equation, were difficult to locate in the literature, and those that were available did not agree throughout the desired temperature range. The viscosity values published in the International Critical Tables appeared to be the most reliable and are presented in table 3. These values are for atmospheric pressure only, and were exclusively used to compute the values of KA/L shown in figure 13 and tables 4 and 5.

RESULTS

The results are presented both in graphical and tabular form in figures 13 to 16 and tables 4 to 7. For purposes of presenting flow-calibration curves for the metering element plots of $Q_m/\Delta P$ against P_m were accomplished for the two temperatures at which tests were made (figs. 14 and 15). The effect of pressure upon the viscosity of air for the two temperature conditions is demonstrated in figure 13 by plotting KA/L against $1/P_m$, wherein the values for the viscosity of air substituted into Darcy's law were those at atmospheric pressure. Finally, computed values for the viscosity of air for the range of

pressures of these tests are shown in figure 16 compared with data for the viscosity of nitrogen taken from reference 8.

As was previously mentioned the initial objective of these tests was to investigate the possibilities of a porous medium to serve as a flow-metering element capable of calibration to 0.1 to 0.2 percent. Probably the primary factor encountered during these tests to prevent attainment of such an accuracy was the inability to maintain absolutely, steady, predetermined temperatures. The greatest such variation in temperature occurred during the low-temperature runs, where no means of controlling thermal conditions was provided. Within the range of these runs, the viscosity of air is known to vary approximately 1 percent. The thermal expansion of the Alundum material, which affects the size of the pores, alters the permeability by approximately 0.06 percent, based on the increase in K_{liq} with temperature, as indicated in figure 13. This latter factor is relatively small and could be ignored. The effect on the results due to the variation in viscosity over the temperature range of these tests is of sufficient magnitude to introduce a serious incompatibility into the results for $Q_m/\Delta P$. No such inconsistencies are involved in the computations for KA/L since the viscosity, corrected for the temperature, is introduced into Darcy's equation to compute this term. In many cases the possible disagreement in values of $Q_m/\Delta P$ due to inability to operate at constant temperatures is eliminated or reduced by averaging the results for runs made at constant pressure, but different temperatures. The mean temperature of operation for the low-temperature runs appears to be approximately 75° F. Only in isolated cases does the average temperature of operation at any pressure vary seriously (in excess of 3° F) from this mean. Notable exceptions are the runs at 400 and 800 pounds per square inch absolute and several runs at low pressures (runs 1-1, 1-3, 1-4, and 1-11). The net effect of this temperature variation on the curve for $Q_m/\Delta P$ against P_m for the low-temperature runs can be predicted to be a maximum possible error of 0.2 percent, if the mean temperature of operation is considered to be 75° F. This type of error is considered negligible in the case of the high-temperature runs because of the better control over the temperature. In any event no similar incompatibilities are involved in the curves for KA/L against $1/P_m$.

METERING OF GASES WITH A POROUS MEDIUM

The operation of the experimental apparatus during the tests of the present investigation appears to indicate that an element of stable porous substance with large area and small thickness will serve ideally as a metering element. In a preliminary investigation, during which

period no data were recorded, a study was made to determine such factors as sensitivity, ease of control, steadiness of flow, and other aspects important to flow metering. The ability of the porous element to reduce any pulsations in the gas flow appeared to be its greatest virtue, a very important factor in accurate metering. At all normal pressure differentials the flow was completely free of any such disturbances, as indicated by the manometer. This property is manifested by the ability of the apparatus to maintain, with steady gas flow, absolutely constant manometer readings for indefinite periods of time. Occasionally when tests were conducted at pressures below 30 pounds per square inch absolute some fluctuation of the manometer columns was noticed. This was attributed to the large rate of change of $Q_m/\Delta P$ with P_m at these low pressures, combined with the inability of the regulators to maintain constant pressures in this range. A slight deviation in the mean pressure produced a considerable change in Q_m .

Because of the linear characteristics of flow through the porous metering element sensitivity and uniformity of control can be maintained at all flow rates. This behavior is in contrast with that of the usual type of flow meter that produces a pressure differential which is a function of the flow rate squared. A serious disadvantage of this latter type of instrument is the low sensitivity at small flow rates. A further disadvantage is the manner in which the discharge coefficient varies with the Reynolds number. Only at values of this parameter in excess of approximately 100,000 does the coefficient of discharge of an orifice-type instrument remain essentially constant, decreasing rapidly with lower Reynolds numbers. Because of the nature of the flow in this region, calibration and use of such an instrument for low flow rates is usually not advised. There appears to be no similar lower limit of applicability of a porous metering element.

As a general comment, a porous metering element is at least as difficult to calibrate as an orifice plate. The advantages of the former are recognized when operated as a laboratory instrument. Its flow characteristics result in excellent range of operation, sensitivity, and accuracy. Relatively little effort is required to manipulate the flow rate because of the linear flow characteristics.

A more complete analysis of the ability of this equipment to meter gas can be obtained through reference to the graphical and tabular results. The calibration curves, figures 14 and 15, indicate without a doubt that satisfactory calibration curves can be obtained with normal laboratory techniques. The proximity of the experimental points to the faired curves suggests that they can be used with considerable confidence. It is encouraging to note that the curves of KA/L against $1/P_m$ (fig. 13) are almost as equally smooth through the experimental points. This form of cross plotting can be used to advantage, especially at the

lower pressures, as a check against possible errors. At pressures below approximately 75 pounds per square inch absolute the use of atmospheric viscosity data will result in a straight-line plot on this latter curve, as originally shown by Klinkenberg.

The shapes of the calibration curves suggest that each metering element of different permeability will possess an optimum pressure range wherein better results should be expected. Referring to figure 14 it is seen that at pressures below 50 pounds per square inch absolute the slope of the curve is large, which indicates that the value of $Q_m/\Delta P$ will vary substantially with small changes of P_m . This behavior imposes the necessity of maintaining very accurate pressure regulation if this element is to be utilized as a flow meter at these low pressures. In contrast with this low-pressure behavior, the curve assumes a very small slope at pressures greater than 300 pounds per square inch absolute, necessitating a high degree of accuracy for the flow-rate measurements, as compared with the accuracy required for the pressure measurements. For this particular element it would appear that it could be used with best results within the pressure range of 50 to 300 pounds per square inch absolute. As a general rule it may be stated that as the calibration curve approaches the $Q_m/\Delta P$ -axis precautions should be taken in the measurement of pressure; as the curve approaches the P_m -axis emphasis should be placed on precision of flow-rate determinations.

With reference to figure 1 it can be shown that this optimum range for measurements will shift toward regions of higher pressure as the permeability of the porous substance decreases. It was seen previously that the slope of the curve of K against $1/P_m$ was constant and increased with reduced pore size or increased mean free path. Thus an element of lower permeability will produce a calibration curve with a greater slope at high pressures, but at the same time increasing the slope of the curve at the lower pressures. Although the element employed in these tests appeared to produce satisfactory results from 16 to 850 pounds per square inch absolute, undoubtedly better results could have been obtained by the use of several elements of different permeability.

The ability of this apparatus to reproduce its results is best demonstrated by reference to the data in table 4 for the low-temperature tests. At all mean pressures of 40 pounds per square inch absolute, and greater, two or more runs were made at varying flow rates, with the plotted results being the average of all the runs at that particular pressure. The consistency of the results at any pressure can be evaluated by observing the variation in the values of $Q_m/\Delta P$ and KA/L . It can be seen that the most consistent results are found in the range 100 to 300 pounds per square inch absolute. At 300 pounds per square inch absolute six runs (runs 47-52) were accomplished with a maximum spread of 0.3 percent in

the values of $Q_m/\Delta P$ and 0.6 percent in the values of KA/L . The probable deviation for these results is 0.08 and 0.16 percent, respectively, for the two values in question. Below 100 or above 300 pounds per square inch absolute the results are not so consistent in several instances. At 600 pounds per square inch absolute (runs 63 to 69) a total spread of 1.5 percent in the values for both $Q_m/\Delta P$ and KA/L is found. The probable error in this case is 0.4 percent for both quantities. Similarly poor results were recorded at 75 pounds per square inch absolute (runs 23 to 29) which show a probable error of 0.35 percent. The probable error for most of the remaining groups of observations is 0.2 percent or less. It is entirely probable that a portion of these errors was introduced because of the lack of absolute temperature controls.

The validity of Darcy's law was verified to the extent of the flow capabilities of the volumetric displacement tank. These results are presented in table 6. Runs were made at pressure differentials up to approximately 24 pounds per square inch. Greater pressure drops were not attempted because of the possibility of rupturing the thimble. It can be seen from these results that the values of $Q_m/\Delta P$ are essentially constant, except for several of the values near the maximum flow rates. It is probable that the results at these large pressure differentials are somewhat in error because of the necessity of observing the manometer by eye, since the differentials were beyond the range of the cathetometer. This reduction in the values of $Q_m/\Delta P$ at the higher flow rates may also be attributed to some oversized capillaries in the Alundum. Such a disparity in the pore size suggests the obvious conclusion that eddies have developed in these larger capillaries, thus reducing the net value of Q_m for any pressure differential. The maximum Reynolds number computed for these tests was 0.0373, indicating that the flow did not depart from the laminar regime, as shown in figure 5. Extrapolation of these results shows that this particular element will pass 130 pounds of air per hour at these conditions of temperature and pressure before approaching the limit of Darcy's law. The capacity of the element increases as the mean pressure increases, this capacity being predictable for any condition by computing the flow to give a Reynolds number of 0.2.

As a summary to the preceding statements it may be concluded that a porous metering element is capable of calibration to 0.1 percent within a range of pressures peculiar to the particular substance employed. Beyond this range the requirements for high precision of flow-rate measurement at the high pressures and for high precision of pressure measurement at the low pressures will make accurate calibration difficult. This difficulty may be averted by employing a number of elements of different permeabilities, each operated only within its optimum pressure range. The calibration of a group of elements under these conditions will require

considerably less effort than attempting to calibrate a single element over a large range of pressure because of the more consistent results probable in the former case. Difficulties necessitated by the calibration will be counteracted by the stability of the flow, high precision, and excellent control characteristics. The linear dependency of flow rate on pressure drop is an invaluable asset.

APPLICATION OF FLOW OF GAS THROUGH POROUS MEDIUM TO
DETERMINATION OF VISCOSITY OF GAS

The Klinkenberg effect for the flow of gas through a porous substance has been discussed in the section entitled "Permeability of Porous Medium to Gases." It will be recalled that the present author showed both analytically and experimentally that the permeability of a porous medium to any gas can be expressed by the relationship

$K = K_{liq} \left[1 + (b/P_m) \right]$, the symbols being as listed. Such a relationship immediately implies that K should vary as the reciprocal mean pressure, and this hypothesis has been well-substantiated by several investigations.

The behavior of K with P_m just described permits the determination of the constant b with reasonable accuracy. If values for K are computed from experimental-flow results and atmospheric-viscosity data the points will plot as a straight line on a plot of K against $1/P_m$ at low pressures and will commence to fall away from this line at higher pressures. This effect is illustrated in figure 13. It is seen therein that at mean pressures above approximately 100 pounds per square inch absolute the use of such viscosity data warps the curve downward from the projected straight line. This indicates that the atmospheric data employed should be corrected for the influence of pressure beyond this point. Below this pressure the viscosity is apparently unaffected by the gas pressure and a valid straight line can be drawn through the points. The dashed projections of the straight segments of the curves indicate their predicted appearance if correct viscosity data had been employed at the higher pressures.

For purposes of determining this probable correct viscosity the equation of flow through a porous medium can be written in the form:

$$\mu = \frac{KA/L}{Q_m/\Delta P} = \frac{(K_{liq}A/L) \left[1 + (b/P_m) \right]}{Q_m/\Delta P} \quad (17)$$

The values $K_{\text{liq}}A/L$ and b are readily determined from the intersections of the projected curves obtained at very low pressures with the ordinate and from the slopes. Thus at the lower temperature,

$$\frac{KA}{L} = 262.0 \left(1 + \frac{4.214}{P_m} \right) \quad (18)$$

and at the higher temperature,

$$\frac{KA}{L} = 269.3 \left(1 + \frac{6.214}{P_m} \right) \quad (19)$$

Inasmuch as $Q_m/\Delta P$ is shown as a function of P_m in figures 14 and 15, equations (17) and (18) actually give the viscosity as a function of the mean pressure. Upon substitution of the commensurate values into these equations the viscosity data shown in figure 16 and table 7 were obtained.

The accuracy of these viscosity data cannot be confirmed since no similar data can be located in the literature for comparison purposes. The results of Michels and Gibson for nitrogen gas (reference 8), shown also in figure 16, were obtained in 1931 by means of a capillary-type viscosimeter. Since the behavior of air is generally similar to that of nitrogen, it might be expected that the curve shapes should be similar. The curves in figure 16 show that the data for these low-temperature tests are not corroborated by the data of Michels and Gibson at the higher pressures. The curve for nitrogen at 77° F indicates an increasing viscosity-pressure coefficient at these pressures, in contrast with the decreasing trend of this coefficient for air found from these tests.

The above discussion suggests that the results found for the viscosity of air at 75° F are probably in some error at pressures over 500 pounds per square inch absolute. There is apparently no argument to refute the viscosity values found for the high-temperature tests. Several investigators, working with different gases, have shown that the viscosity-pressure coefficient approaches linearity as the temperature is increased. Recent data obtained by Sage and Lacey for methane (reference 9) show that at 100° F this gas produces a viscosity-pressure curve that is slightly concave downward, while at 220° F the relationship is essentially linear, for pressures below 1000 pounds per square inch absolute. Earlier data by Phillips (reference 10) indicate that the viscosity of carbon dioxide is a linear function of pressure in the

temperature range 68° to 104° F and at pressures below the critical value. Additional information is given in reference 11. All data in the literature indicate that the slope of the viscosity-pressure curve decreases as the temperature is increased. It is seen in figure 16 that the data from these tests at 517° F agree with the general trends mentioned above.

EFFECT OF TEMPERATURE ON PERMEABILITY OF ALUNDUM

The thermal effects on the Alundum employed as the metering element can be demonstrated by reference to figure 13. It can be seen that the true permeability of this substance at approximately 517° F is 2.79 percent higher than the corresponding value at approximately 75° F. If the flow is assumed to be proportional to the mean pore diameter squared, and the pores are assumed to increase in proportion to the temperature increase, then this increase in K_{liq} with temperature is equivalent to a thermal expansion of 0.000034 per $^{\circ}$ F. The specifications for the Alundum indicate a thermal coefficient of approximately 0.000004 per $^{\circ}$ F, or approximately one-tenth of the apparent value. These values suggest that the permeability of Alundum increases considerably more with temperature than is indicated by the thermal-expansion characteristics. Calhoun and Yuster predicted an increase in permeability with temperature, but found experimentally that the permeability of silica cores was unchanged with water in the range 0° to 60° C. For an equal temperature range Alundum would show only a 0.7-percent increase in permeability, which is comparable with the accuracy of their results. It is entirely possible that the small temperature range covered by these authors did not permit an evaluation of this effect. This analysis appears to indicate that the expansion characteristics of a porous material will not serve as criteria for predicting the change of permeability with temperature. The results of Calhoun and Yuster, Grunberg and Nissan, and of these tests suggest that each porous substance may have a permeability-temperature characteristic peculiar to that material.

The shapes of the two curves in figure 13 substantiate the hypothesis of Klinkenberg that the constant b in the equation

$$K = K_{liq} \left[1 + (b/P_m) \right]$$

is a function of the mean free path of the gas.

Molecular density of an unconfined gas decreases with temperature, and the kinetic theory shows that the mean free path is inversely proportional to the density. A qualitative discussion of this influence is not possible because of the complexity of the combined effects of temperature upon viscosity, coefficient of friction, and the radius of the capillaries.

CONTAMINATION OF POROUS METERING MATERIAL

In experimentation involving porous metering materials considerable care must be exercised in maintaining the interstices free of contaminants. Any substance that is allowed to enter the capillary passages will have a plugging effect that will result in a reduction of the porosity of the metering material. The two most serious offenders in this respect appear to be liquids and small particles, such as dust, that may pass through the fluid system and be collected by the porous substance. Owing to the great absorptive ability of materials that are suitable for porous metering elements, contamination due to liquids undoubtedly presents the greatest problem. It is doubtful that dry dust particles can reduce the effective flow area of a large thimble. Inasmuch as the interstices of any porous metering substance will be of the order of a 10-micron diameter, the entrance of dust particles into the minute passages appears unlikely.

During these tests the filtering and drying assembly was maintained in position at all times to eliminate contamination of the thimble by any substance entrained in the air. The data shown in figure 12 and tables 4 to 6 were taken without removal of either the thimble or the filtering unit for inspection or servicing. During this period it is estimated that a minimum of 10,000 cubic feet of air was passed through the thimble. At frequent intervals the calibration at 100 pounds per square inch absolute was checked to ascertain the possibility of changing flow characteristics of the Alundum. These check runs produced data that were as consistent as the data from the original series of runs at this pressure that were taken over a period of several days early in the program. This type of measure appeared to be the most appropriate for indicating possible plugging of the thimble.

Upon completion of the tests the Alundum thimble was removed for visual inspection. The original white surface of the thimble was found to be discolored by corrosion particles from the inside surface of the metering case. The corrosion of the metal surface was attributed to a small quantity of mercury that had accidentally entered the metering system from the manometer prior to commencement of the test runs. Although an attempt was made immediately to remove this mercury, apparently a sufficient quantity adhered to the metal to result in mild corrosion during the test program. Inasmuch as the metering case material was stainless steel, the corrosion probably occurred during the high-temperature runs, when the assembly was heated to temperatures as high as 800° F.

The contamination mentioned above was in no manner superficial inasmuch as repeated scrubblings with various solvents failed to remove the

discoloration. Regardless of the nature of the contamination, it introduced no discrepancies into the test results within the limitations of the instruments. This experience indicates that a moderate amount of dry foreign substance can be tolerated in the flow system without altering the calibration characteristics of the porous substance.

C O N C L U S I O N S

The following conclusions are drawn from an investigation of the use of a consolidated porous medium for measurement of flow rate and viscosity of gases at elevated pressures and temperatures.

1. A single Alundum porous element can be calibrated to meter gas with an accuracy between 0.1 and 0.2 percent over an optimum range of mean-flow pressures peculiar to the permeability of the substance.
2. At mean pressures outside of this optimum range the calibration accuracy will diminish because of the requirements of high-precision measurements of either flow rate or mean pressure.
3. Precision gas-flow measurements over a wide range of pressure can be expeditiously accomplished by the use of a series of porous elements, each operated within its optimum pressure range.
4. The use of a porous medium as a gas-metering device offers several attractions, such as linear control characteristics, low pressure drop, uniform flow, and accuracy, that make it a valuable laboratory instrument.
5. The results of gas-flow tests on a porous medium can be applied to compute the viscosity of the flowing gas over a range of pressures and temperatures corresponding to those of the flow tests.
6. The present laboratory procedures and equipment, which were developed primarily for flow-metering purposes, should be modified if utilized solely for viscosity measurements. Such modifications and the perfection of laboratory techniques will probably permit rapid and accurate gas-viscosity determinations over wide ranges of temperature and pressure.

University of California
Berkeley, Calif., October 9, 1950

REFERENCES

1. Klinkenberg, L. J.: The Permeability of Porous Media to Liquids and Gases. *Drilling and Production Practice*, 1941, pp. 200-213.
2. Muskat, M.: *The Flow of Homogeneous Fluids through Porous Media*. McGraw-Hill Book Co., Inc., 1937.
3. Calhoun, J. C., and Yuster, S. T.: A Study of the Flow of Homogeneous Fluids through Ideal Porous Media. *Drilling and Production Practice*, 1946, pp. 200-213.
4. Grunberg, L., and Nissan, A. H.: The Permeability of Porous Solids to Gases and Liquids. *Jour. Inst. Petroleum Tech.*, vol. 29, no. 236, Aug. 1943, pp. 193-225.
5. Gerhart, R. V., Brunner, F. C., Mickley, H. S., Sage, B. H., and Lacey, W. N.: Thermodynamic Properties of Air. *Mech. Eng.*, vol. 64, no. 4, April 1942, pp. 270-272.
6. Crown, J. C.: The Flow of Gas Characterized by the Beattie-Bridgeman Equation of State and Variable Specific Heats. Memo. No. 9619, Naval Ord. Lab., April 1949.
7. Washburn, Edward W., ed.: *International Critical Tables*. Vol. III. First ed., McGraw-Hill Book Co., Inc., 1928.
8. Michels, A., and Gibson, R. O.: The Measurement of the Viscosity of Gases at High Pressures. *Proc. Roy. Soc. (London)*, ser. A, vol. 134, no. 823, Nov. 3, 1931, pp. 288-307.
9. Sage, B. H., and Lacey, W. N.: Effect of Pressure upon Viscosity of Methane and Two Natural Gases. *Trans. Am. Inst. Min. and Met. Eng.*, vol. 127, 1938, pp. 118-134.
10. Phillips, P.: The Viscosity of Carbon Dioxide. *Proc. Roy. Soc. (London)*, ser. A, vol. 87, no. 592, April 18, 1912, pp. 48-61.
11. Comings, E. W., and Egly, R. S.: Viscosity of Gases and Vapors at High Pressures. *Ind. and Eng. Chem.*, vol. 32, no. 5, May 1940, pp. 714-718.

TABLE 1.- PRESSURE, SPECIFIC VOLUME, AND TEMPERATURE RELATIONSHIPS FOR AIR

[Values taken from reference 5]

Pressure (psia)	Specific volume (cu ft/lb) at -								
	70° F	130° F	190° F	250° F	310° F	370° F	430° F	490° F	550° F
25	7.845	8.737	9.628	10.52	11.41	12.30	13.19	14.08	14.97
50	3.921	4.368	4.815	5.261	5.707	6.153	6.599	7.044	7.490
75	2.613	2.912	3.210	3.509	3.807	4.104	4.401	4.699	4.996
100	1.958	2.183	2.408	2.633	2.856	3.080	3.303	3.526	3.750
150	1.304	1.456	1.606	1.756	1.906	2.056	2.205	2.354	2.503
200	.9774	1.091	1.205	1.318	1.431	1.544	1.656	1.768	1.880
300	.6503	.7274	.8036	.8802	.9558	1.031	1.107	1.182	1.256
400	.4869	.5454	.6033	.6612	.7183	.7753	.8323	.8840	.9448
500	.3887	.4363	.4832	.5298	.5759	.6217	.6672	.7126	.7579
750	.2585	.2912	.3231	.3548	.3859	.4168	.4475	.4783	.5087
1000	.1937	.2189	.2434	.2675	.2912	.3147	.3380	.3611	.3840



TABLE 2.- DENSITY OF MERCURY CORRECTED FOR DENSITY OF AIR

Pressure (psia)	Density (g/cc) at -								
	69.8° F	71.6° F	73.4° F	75.2° F	77.0° F	78.8° F	80.6° F	82.4° F	84.2° F
14.7	13.5422	13.5397	13.5373	13.5348	13.5324	13.5299	13.5275	13.5250	13.5216
25	13.5414	13.5389	13.5365	13.5340	13.5316	13.5291	13.5267	13.5242	13.5218
50	13.5394	13.5370	13.5345	13.5321	13.5297	13.5272	13.5248	13.5223	13.5199
100	13.5355	13.5330	13.5307	13.5282	13.5259	13.5234	13.5210	13.5185	13.5161
200	13.5277	13.5252	13.5229	13.5204	13.5181	13.5156	13.5133	13.5108	13.5085
300	13.5199	13.5174	13.5150	13.5125	13.5101	13.5076	13.5052	13.5033	13.5010
400	13.5119	13.5095	13.5070	13.5048	13.5025	13.5001	13.4978	13.4954	13.4931
500	13.5039	13.5016	13.4994	13.4978	13.4949	13.4925	13.4902	13.4878	13.4855
600	13.4961	13.4938	13.4916	13.4893	13.4871	13.4848	13.4825	13.4802	13.4780
700	13.4881	13.4858	13.4836	13.4813	13.4791	13.4768	13.4746	13.4723	13.4700
800	13.4804	13.4781	13.4761	13.4738	13.4716	13.4693	13.4670	13.4643	13.4621
900	13.4721	13.4699	13.4679	13.4657	13.4635	13.4612	13.4590	13.4567	13.4545
1000	13.4639	13.4616	13.4596	13.4573	13.4553	13.4531	13.4510	13.4490	13.4468

TABLE 3.- VISCOSITY OF AIR AT ATMOSPHERIC PRESSURE

[Values taken from reference 7]

Temperature (°F)	Viscosity (micropoises)	Temperature (°F)	Viscosity (micropoises)
32	170.9	464	273.3
50	175.9	482	277.0
68	180.8	500	280.6
86	185.6	518	284.2
104	190.4	536	287.7
122	195.1	554	291.2
140	199.7	572	294.6
158	204.3	590	298.0
176	208.8	608	301.4
194	213.2	626	304.7
212	217.5	644	308.0
230	221.8	662	311.3
248	226.0	680	314.6
266	230.2	698	317.9
284	234.4	716	321.2
302	238.5	734	324.5
320	242.5	752	327.7
338	246.5	770	330.9
356	250.5	788	334.0
374	254.4	806	337.1
392	258.2	824	340.2
410	262.0	842	343.3
428	265.8	860	346.3
446	269.6	878	349.3

TABLE 4.- EXPERIMENTAL RESULTS, LOW-TEMPERATURE TESTS

Run	P _m (psia)	T _m (°F)	ΔP (psi)	Q _m (cu ft/sec)	Q _m /ΔP	KA/L (millidarcys × feet)
1-1	16.17	71.4	3.1122	4.106 × 10 ⁻³	1.319 × 10 ⁻³	328.2
1-2	16.26	72.1	3.1842	4.214	1.323	329.1
1-3	17.14	71.4	5.0289	6.597	1.312	325.8
1-4	17.81	71.4	5.8411	7.599	1.301	323.0
1-5	18.65	73.2	6.5901	8.476	1.286	320.4
1-6	20.18	72.9	7.8651	9.937	1.263	315.0
1-7	21.73	73.2	5.6417	7.056	1.251	312.0
1-8	23.15	72.0	5.1511	6.400	1.242	308.9
1-9	23.76	72.5	7.0674	8.727	1.235	307.7
1-10	24.71	73.6	7.7511	9.477	1.223	305.2
1-11	26.22	71.4	5.1554	6.305	1.222	304.0
1-12	27.39	72.0	6.0014	7.268	1.211	301.4
1-13	30.73	72.9	6.5245	7.775	1.192	297.4
1-14	34.15	72.9	6.8427	8.075	1.180	294.1
1-15	40.00	74.8	6.5393	7.534	1.152	288.0
1-16	40.00	74.8	7.3784	8.538	1.156	289.0
1-17	40.00	74.8	7.9163	9.174	1.159	289.9
1-18	50.00	73.2	5.8679	6.689	1.139	284.1
1-19	50.00	77.2	8.4174	9.536	1.132	283.4
1-20	60.00	73.2	2.9624	3.335	1.126	280.7
1-21	60.00	73.2	4.5611	5.135	1.126	280.7
1-22	60.00	73.2	6.6690	7.479	1.122	279.9
1-23	75.00	75.0	1.3699	1.526	1.115	278.9
1-24	75.00	75.0	3.4564	3.844	1.112	278.2
1-25	75.00	75.4	5.2433	5.819	1.110	277.8
1-26	75.00	73.6	5.9166	6.539	1.105	275.8
1-27	75.00	73.6	6.6798	7.375	1.104	275.4
1-28	75.00	75.4	7.1164	7.924	1.113	278.4
1-29	75.00	73.6	8.5696	9.459	1.104	275.4
1-30	100.0	73.6	4.0194	4.404	1.095	273.0
1-31	100.0	73.6	4.5165	4.937	1.093	272.8
1-32	100.0	73.6	5.0490	5.508	1.091	272.4
1-33	100.0	73.6	5.6690	6.201	1.093	272.8
1-34	100.0	73.6	6.2947	6.858	1.089	271.8
1-35	100.0	73.6	6.9115	7.577	1.096	273.5
1-36	100.0	73.6	7.7161	8.413	1.090	272.2
1-37	100.0	73.6	8.4940	9.250	1.089	272.0
1-38	100.0	73.6	9.2289	10.06	1.091	272.4
1-39	150.0	76.5	4.0242	4.296	1.068	267.2
1-40	150.0	74.8	5.2800	5.613	1.067	266.9
1-41	150.0	76.5	5.3904	5.749	1.067	267.4
1-42	150.0	74.8	6.3241	6.725	1.064	266.2
1-43	200.0	77.9	1.0080	1.060	1.051	263.8
1-44	200.0	78.2	2.2069	2.327	1.054	264.7
1-45	200.0	78.3	3.3328	3.510	1.053	264.5
1-46	200.0	78.2	4.7891	5.039	1.052	264.3
1-47	300.0	76.1	1.0171	1.053	1.035	259.4
1-48	300.0	76.1	1.7953	1.854	1.033	258.9
1-49	300.0	78.2	2.6764	2.772	1.036	260.1
1-50	300.0	75.4	2.8454	2.941	1.034	258.4
1-51	300.0	78.2	3.8227	3.954	1.034	259.6
1-52	300.0	76.1	3.9593	4.095	1.034	258.7
1-53	400.0	78.9	.8685	.8866	1.021	256.6
1-54	400.0	80.0	1.5266	1.565	1.025	258.0
1-55	400.0	80.0	2.3530	2.402	1.021	257.0
1-56	400.0	80.0	3.1409	3.198	1.018	256.3
1-57	500.0	71.8	.5397	.5493	1.018	253.3
1-58	500.0	77.2	.7287	.7412	1.017	254.9
1-59	500.0	71.8	1.0550	1.066	1.011	251.6
1-60	500.0	77.2	1.5650	1.582	1.011	253.5
1-61	500.0	71.8	1.7215	1.746	1.014	252.3
1-62	500.0	77.2	2.1063	2.130	1.011	253.5
1-63	600.0	73.6	.5486	.5559	1.010	252.1
1-64	600.0	73.6	.8842	.8970	1.014	253.1
1-65	600.0	73.6	1.1239	1.145	1.015	253.3
1-66	600.0	73.6	1.4735	1.482	1.003	250.2
1-67	600.0	75.0	1.6323	1.643	1.006	251.6
1-68	600.0	73.6	1.8418	1.849	1.001	249.7
1-69	600.0	73.6	2.2052	2.211	1.000	249.5
1-70	700.0	75.4	.6388	.6391	1.001	250.5
1-71	700.0	72.9	.7900	.7916	1.002	249.5
1-72	700.0	77.2	.8187	.8208	1.003	251.6
1-73	700.0	72.9	.9797	.9794	1.000	249.1
1-74	700.0	72.9	1.1674	1.169	1.002	249.5
1-75	700.0	77.3	1.7741	1.780	1.003	251.6
1-76	800.0	73.2	.5189	.5210	1.004	250.5
1-77	800.0	77.2	.5209	.5172	.993	249.1
1-78	800.0	75.4	.7104	.7073	.996	249.3
1-79	800.0	73.2	.8850	.8847	1.000	249.5
1-80	800.0	77.2	1.0414	1.039	.998	250.3
1-81	800.0	75.4	1.2656	1.263	.998	249.8
1-82	850.0	72.8	.2813	.2806	.997	248.3
1-83	850.0	72.8	.6846	.6846	1.000	249.1
1-84	850.0	71.8	1.2635	1.263	.996	247.9
1-85	850.0	71.8	1.4789	1.477	.998	248.3



TABLE 5.- EXPERIMENTAL RESULTS, HIGH-TEMPERATURE TESTS

Run	P_m (psia)	T_m (°F)	ΔP (psi)	Q_m (cu ft/sec)	$Q_m/\Delta P$	KA/L (millidarcys × feet)
2-1	19.93	517.0	9.8371	0.8911×10^{-3}	0.906×10^{-3}	352.3
2-2	23.04	517.2	15.530	1.360	.876	340.1
2-3	27.36	516.7	22.817	1.944	.852	331.0
2-4	32.84	516.0	5.7998	.4793	.826	320.9
2-5	43.35	516.0	7.5385	.5947	.789	306.8
2-6	50.00	516.3	8.0352	.6263	.779	302.8
2-7	67.83	516.0	6.4859	.4901	.756	293.7
2-8	104.6	516.2	7.6857	.5647	.735	285.4
2-9	200.0	516.0	6.2597	.4443	.710	275.8
2-10	300.9	516.8	2.6960	.1890	.701	272.5
2-11	506.9	516.0	1.3109	.09092	.694	269.5
2-12	752.4	516.0	1.2047	.08287	.689	267.1



TABLE 6.- EXPERIMENTAL RESULTS, LINEARITY OF DARCY'S LAW

Run	P_m (psia)	T_m (°F)	ΔP (psi)	Q_m (cu ft/sec)	$Q_m/\Delta P$	Reynolds number
3-1	50.00	73.2	2.953	3.340×10^{-3}	1.131×10^{-3}	0.00470
3-2	50.00	73.2	3.934	4.445	1.130	.00623
3-3	50.00	73.2	4.879	5.520	1.131	.00775
3-4	50.00	73.2	5.867	6.636	1.131	.00930
3-5	50.00	73.2	6.816	7.730	1.134	.0108
3-6	50.00	73.2	7.878	8.918	1.132	.0125
3-7	50.00	73.2	8.924	10.08	1.130	.0141
3-8	50.00	73.2	9.861	11.16	1.132	.0157
3-9	50.00	73.2	11.13	12.47	1.131	.0175
3-10	50.00	73.2	11.25	12.70	1.129	.0178
3-11	50.00	73.2	12.23	13.82	1.130	.0194
3-12	50.00	73.2	12.86	14.58	1.133	.0204
3-13	50.00	73.2	13.54	15.40	1.138	.0216
3-14	50.00	73.2	14.61	16.53	1.132	.0232
3-15	50.00	73.2	15.25	17.21	1.129	.0242
3-16	50.00	73.2	16.38	18.51	1.130	.0260
3-17	50.00	73.2	17.42	19.72	1.132	.0276
3-18	50.00	73.2	17.52	19.70	1.125	.0276
3-19	50.00	73.2	17.88	19.95	1.116	.0280
3-20	50.00	73.2	17.98	20.20	1.124	.0284
3-21	50.00	73.2	19.86	22.44	1.129	.0315
3-22	50.00	73.2	23.67	26.63	1.125	.0373

TABLE 7.- VISCOSITY OF AIR

Pressure (psia)	Viscosity (micropoises) at -	
	75° F	517° F
100	182.9	284.0
200	185.7	285.0
300	187.7	285.3
400	189.4	286.0
500	190.7	286.8
600	192.0	287.0
700	192.8	287.8
800	193.4	288.4
900	193.7	-----



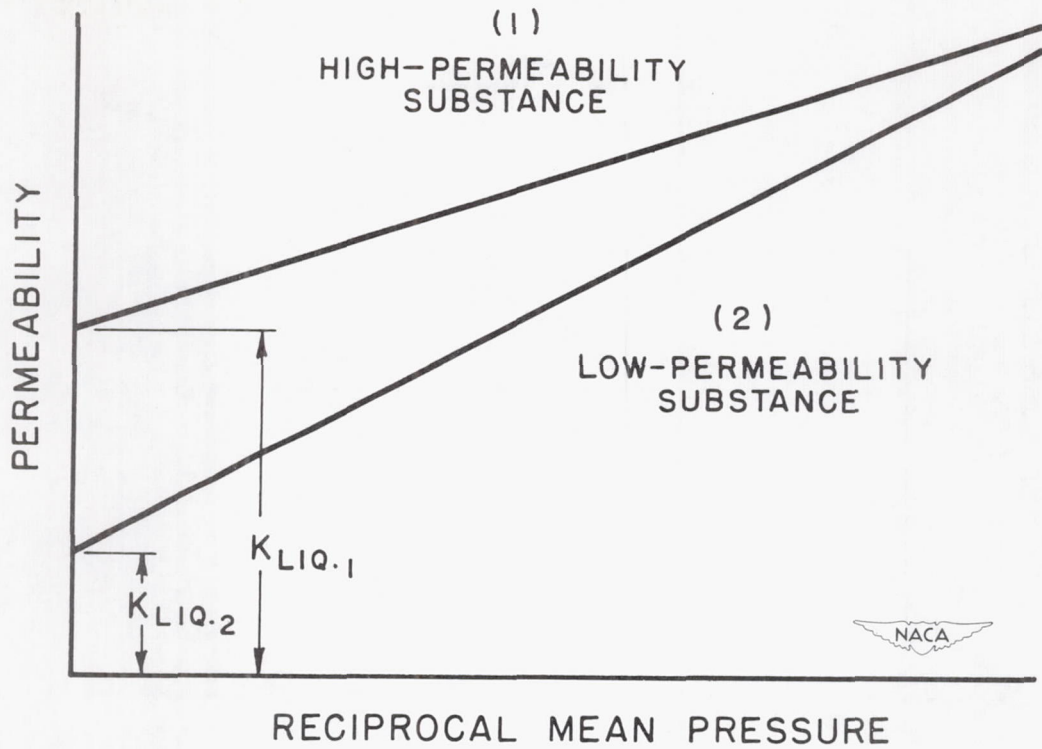


Figure 1.- Reciprocal mean pressure against permeability for high- and low-permeability substances.

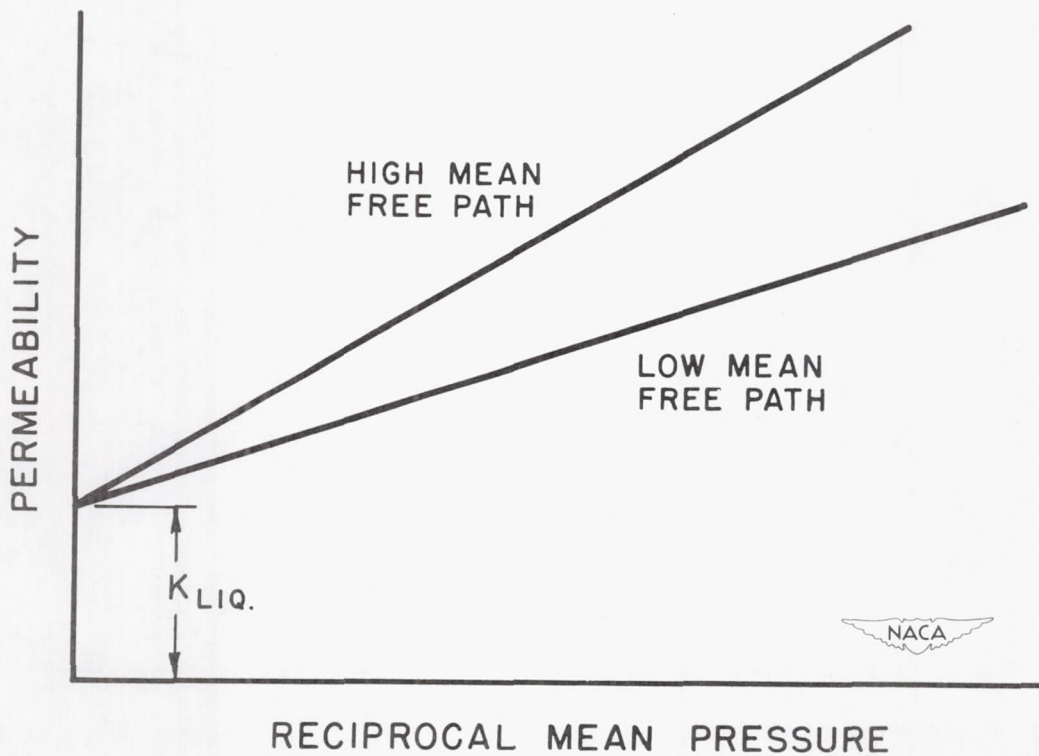


Figure 2.- Reciprocal mean pressure against permeability for high and low mean free paths.

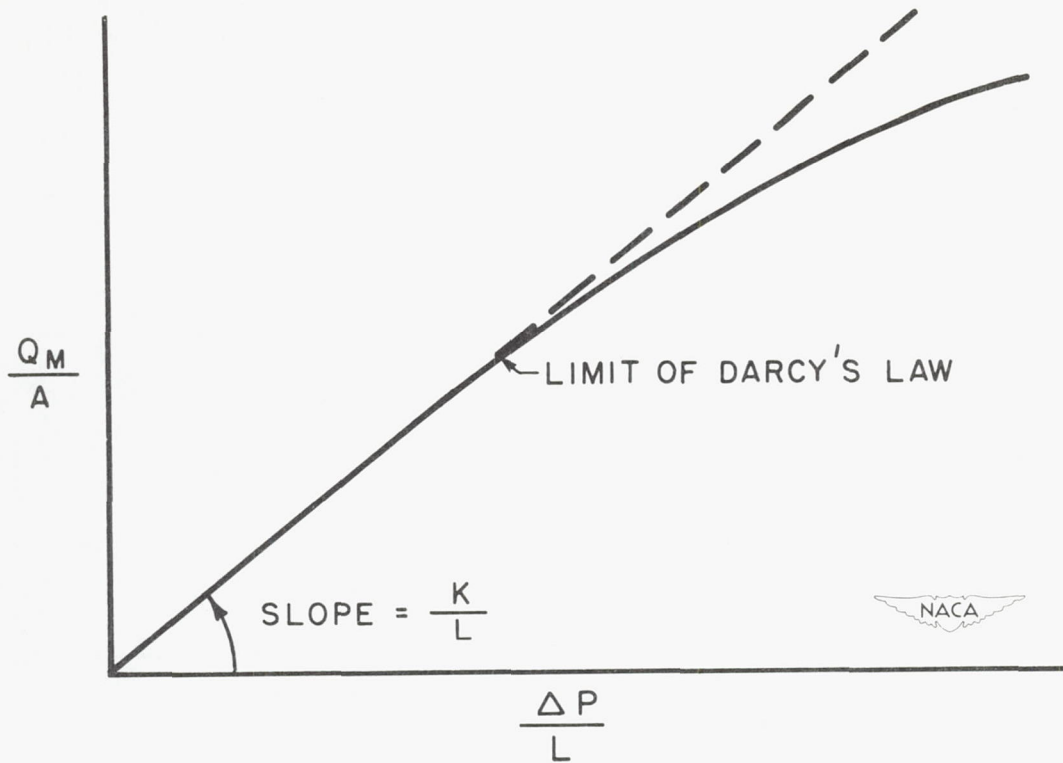


Figure 3.- Q_m/A against $\Delta P/L$ plotted on rectangular coordinates.

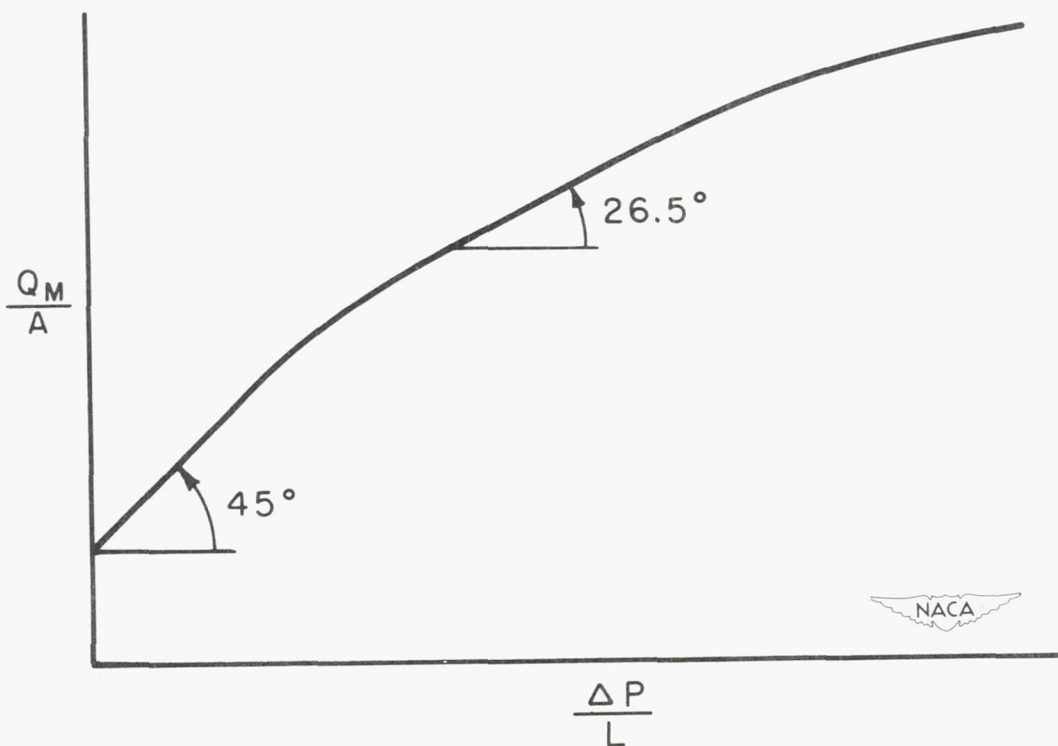


Figure 4.- Q_m/A against $\Delta P/L$ plotted on logarithmic coordinates.

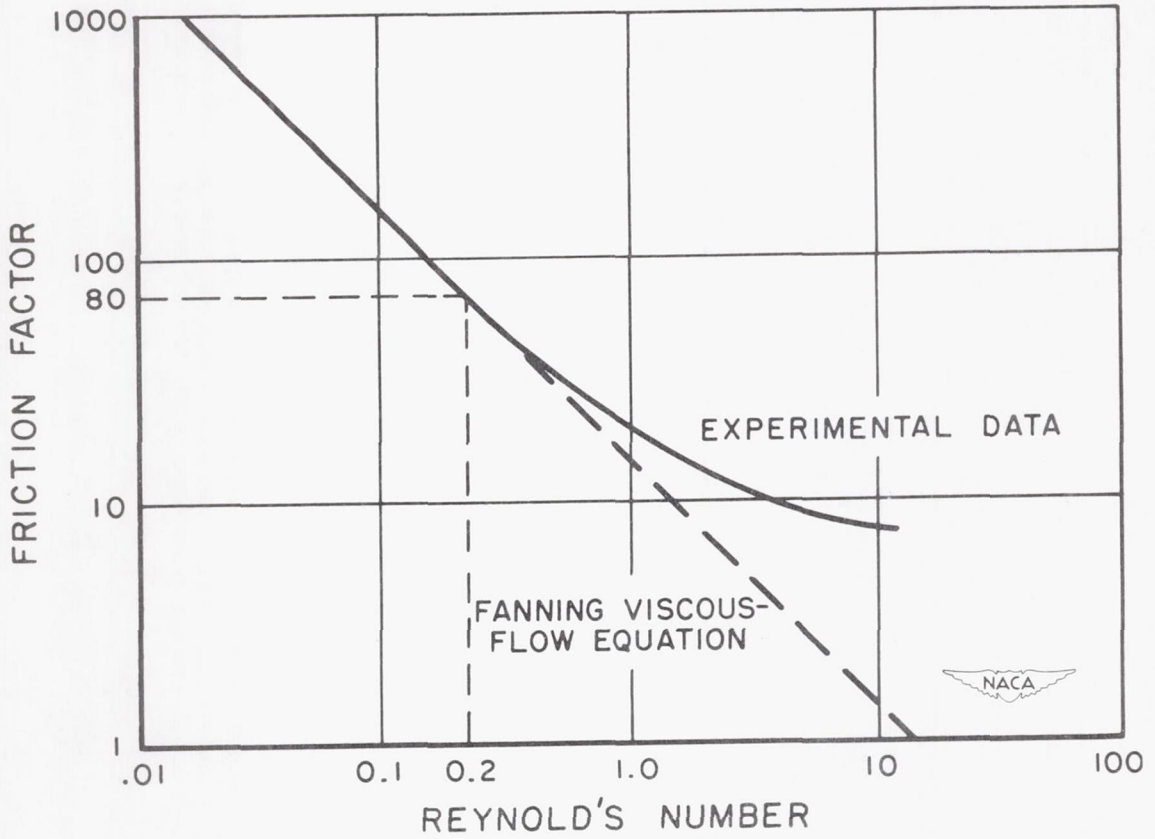


Figure 5.- Friction factor against Reynolds number.

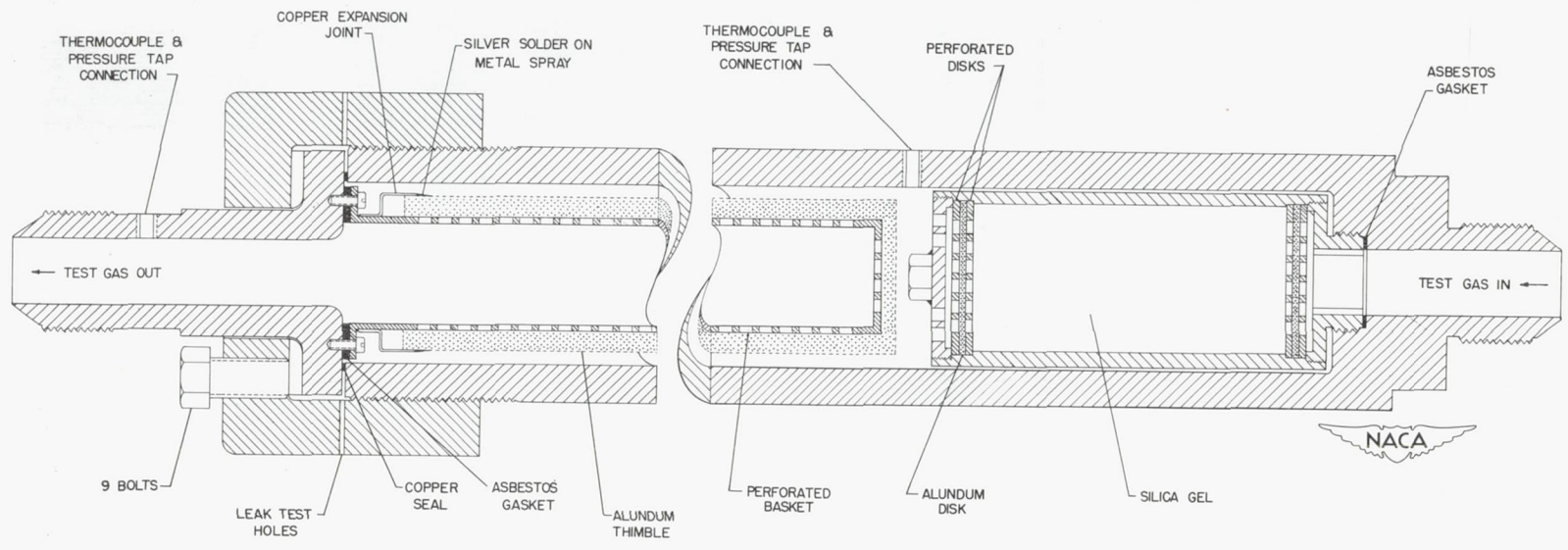


Figure 6.- Flow meter.

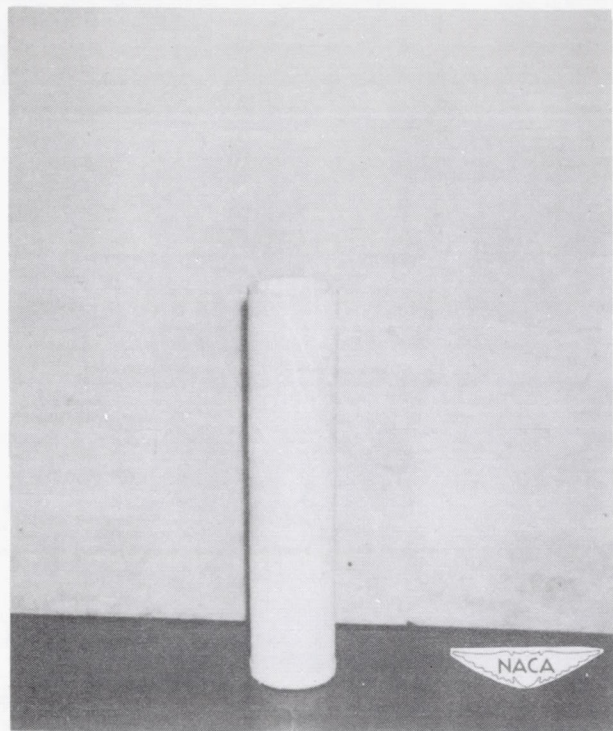


Figure 7.- Unmounted thimble.

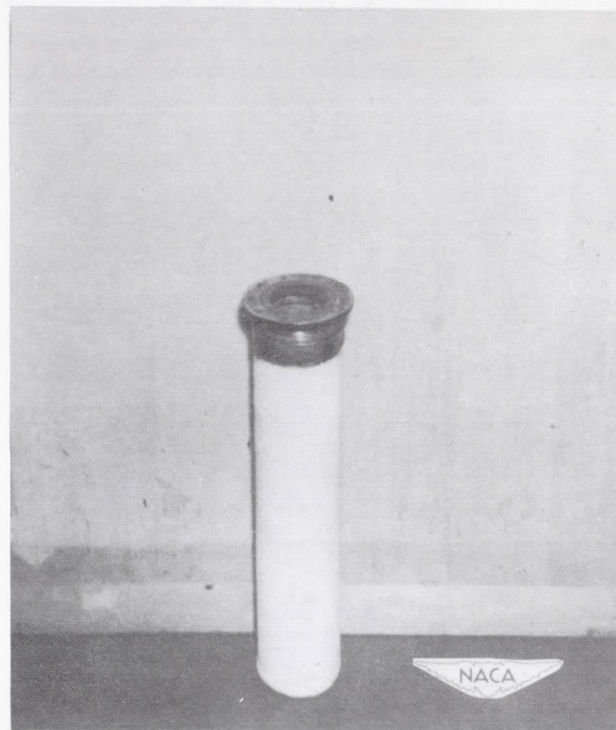


Figure 8.- Mounted thimble.

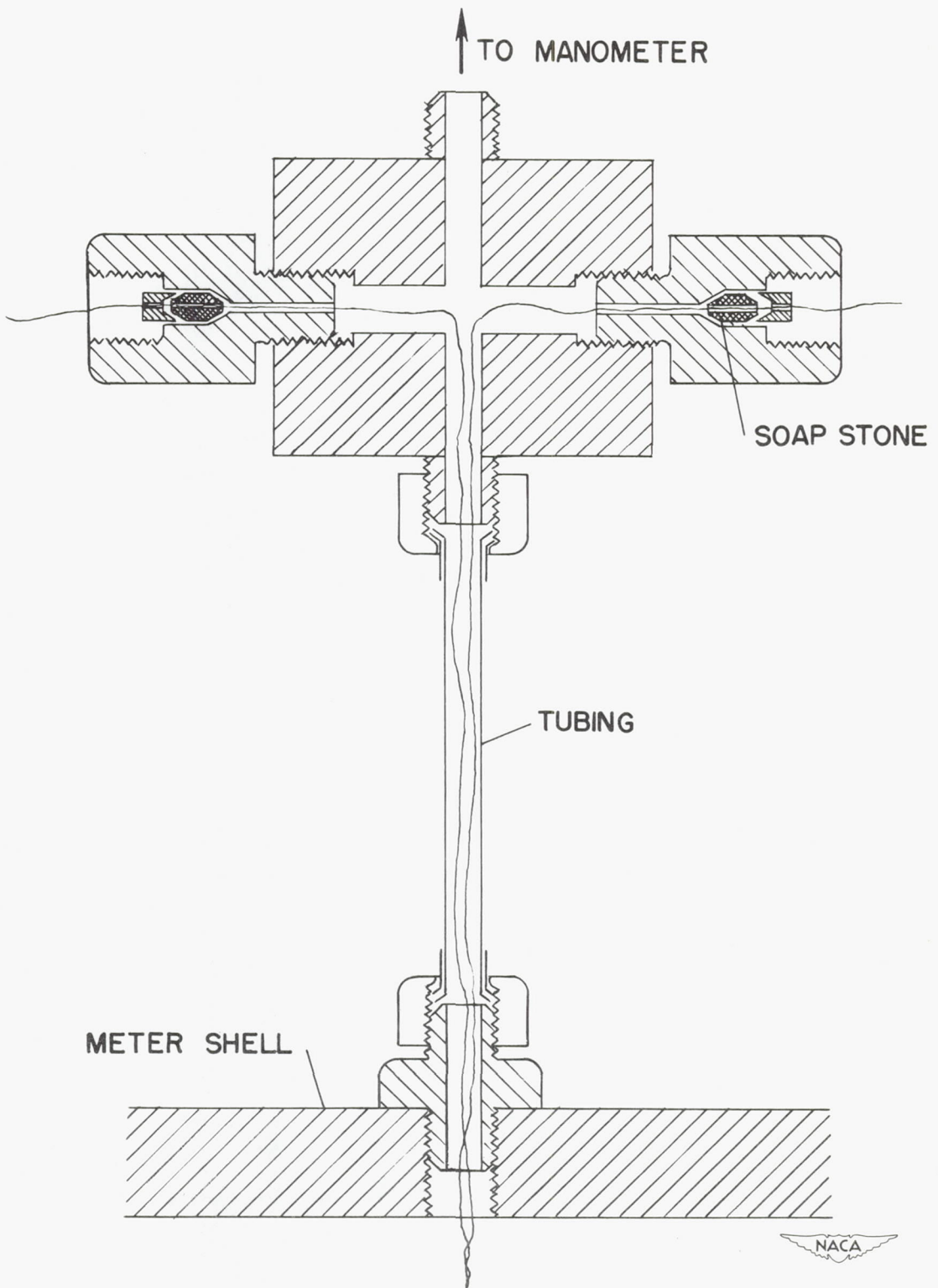


Figure 9.- Adapter for thermocouple and manometer connection.

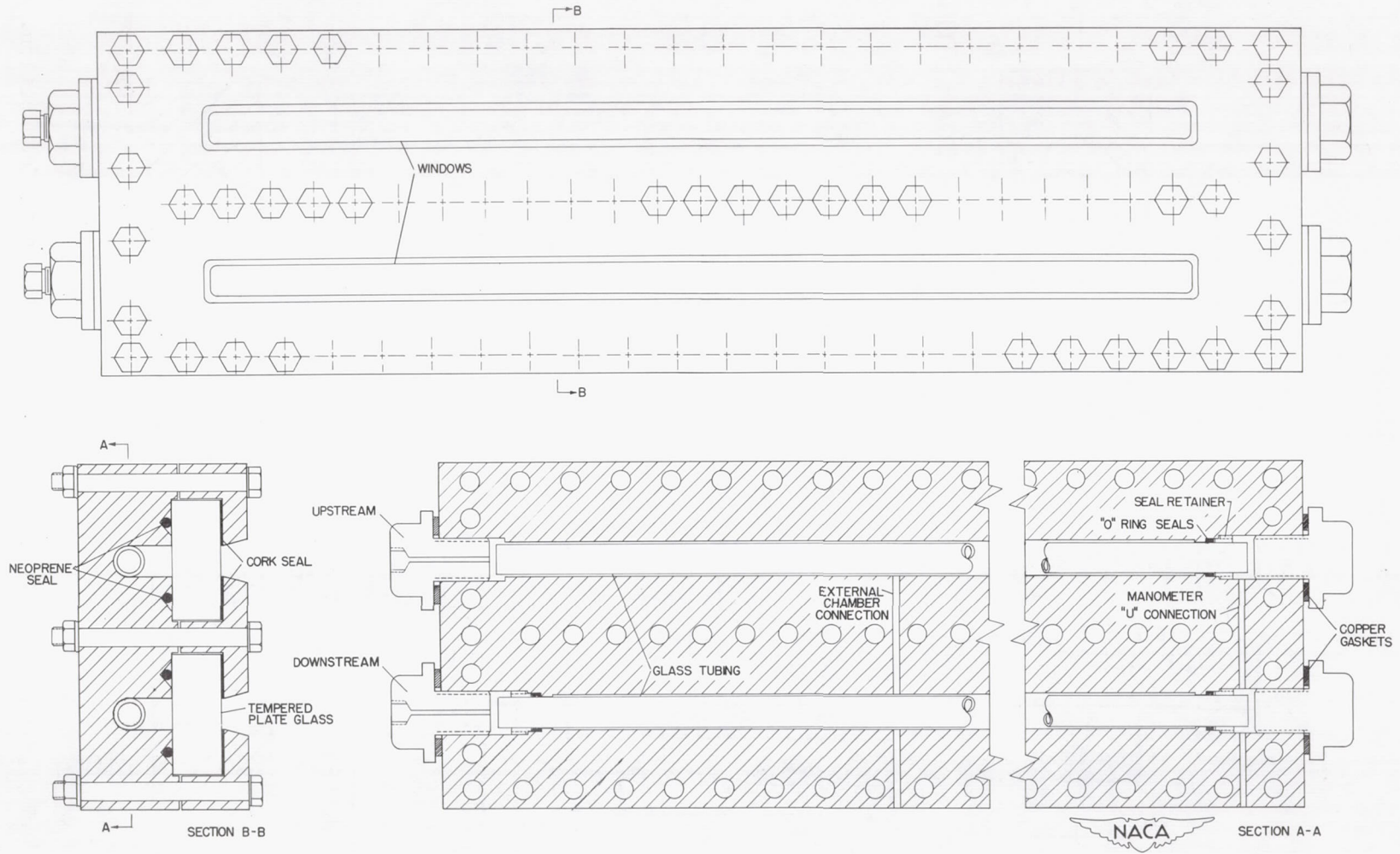


Figure 10.- High-pressure manometer.

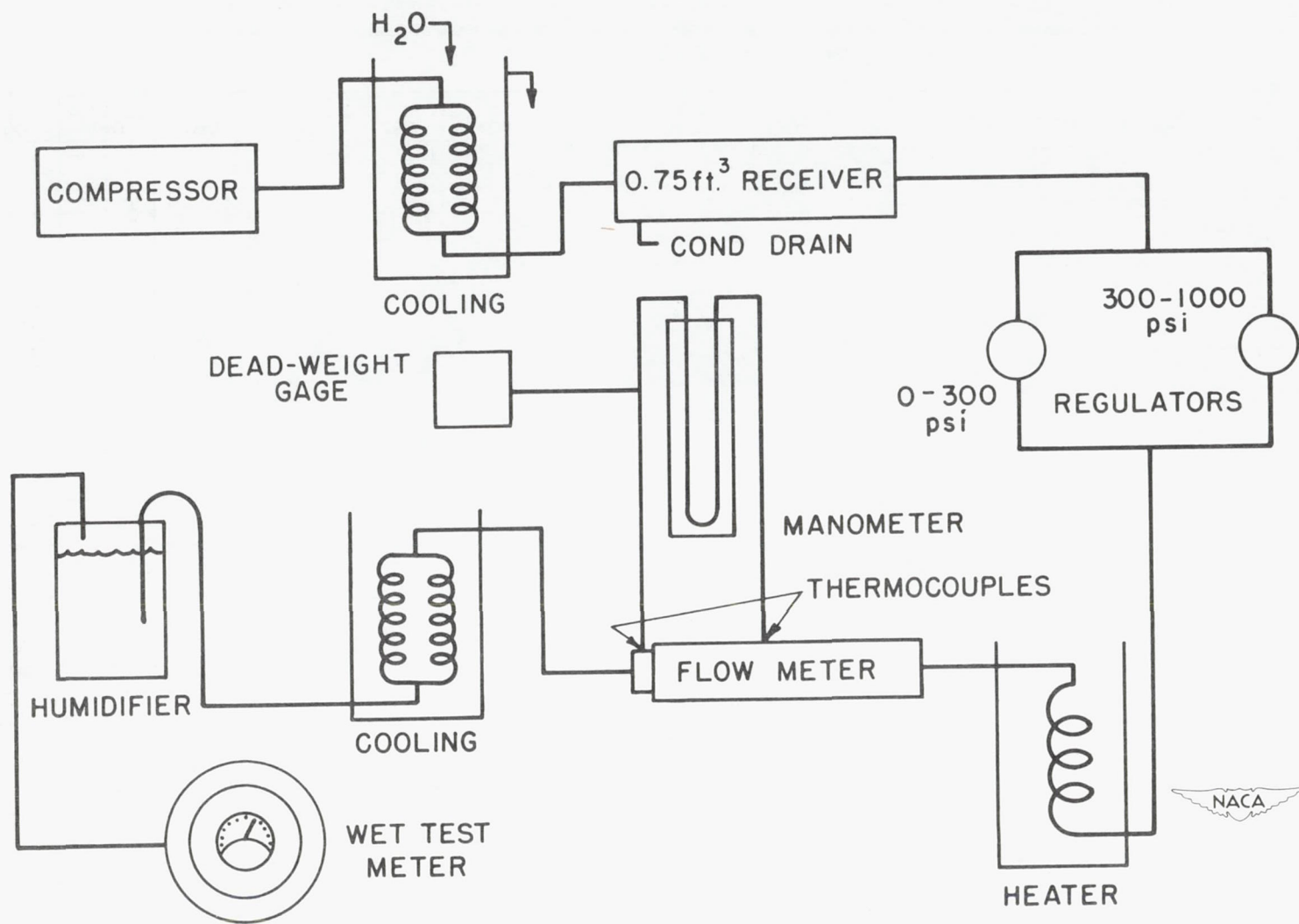


Figure 11.- Schematic flow diagram.

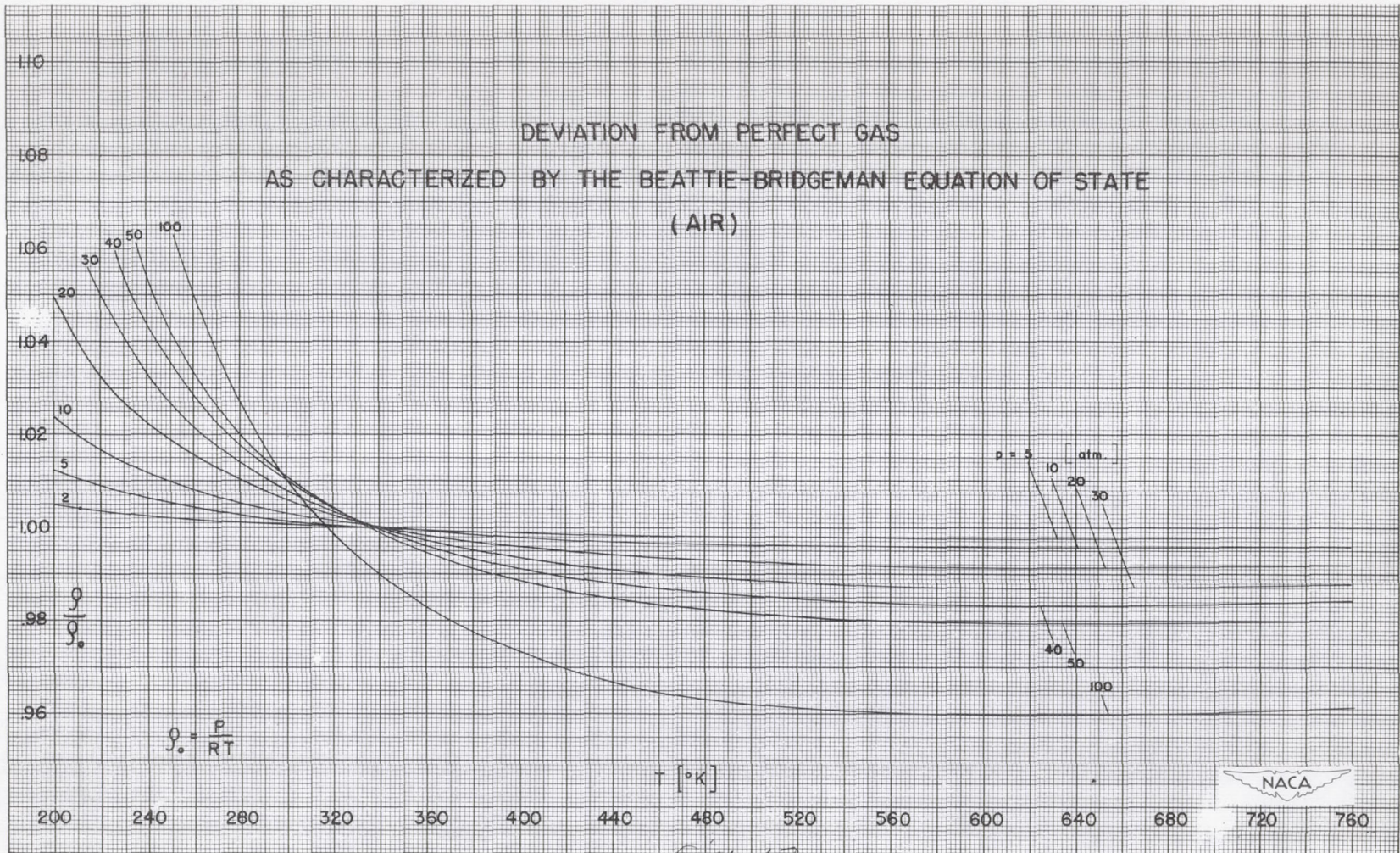


Figure 12.- Deviation from perfect gas as characterized by Beattie-Bridgeman equation of state. Medium used is air. $\rho_0 = P/RT$.

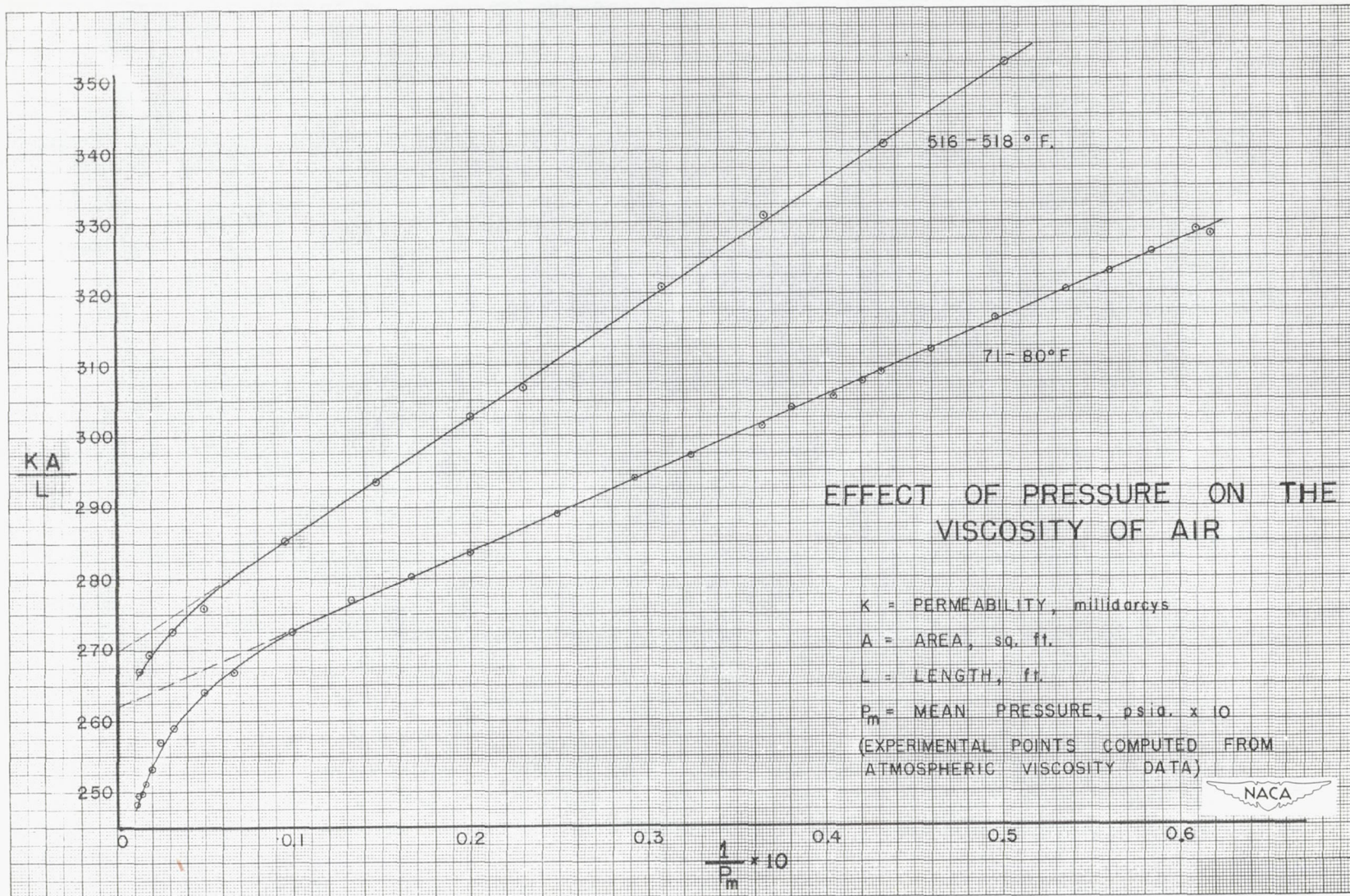


Figure 13.- Effect of pressure on viscosity of air. Experimental points computed from atmospheric viscosity data.

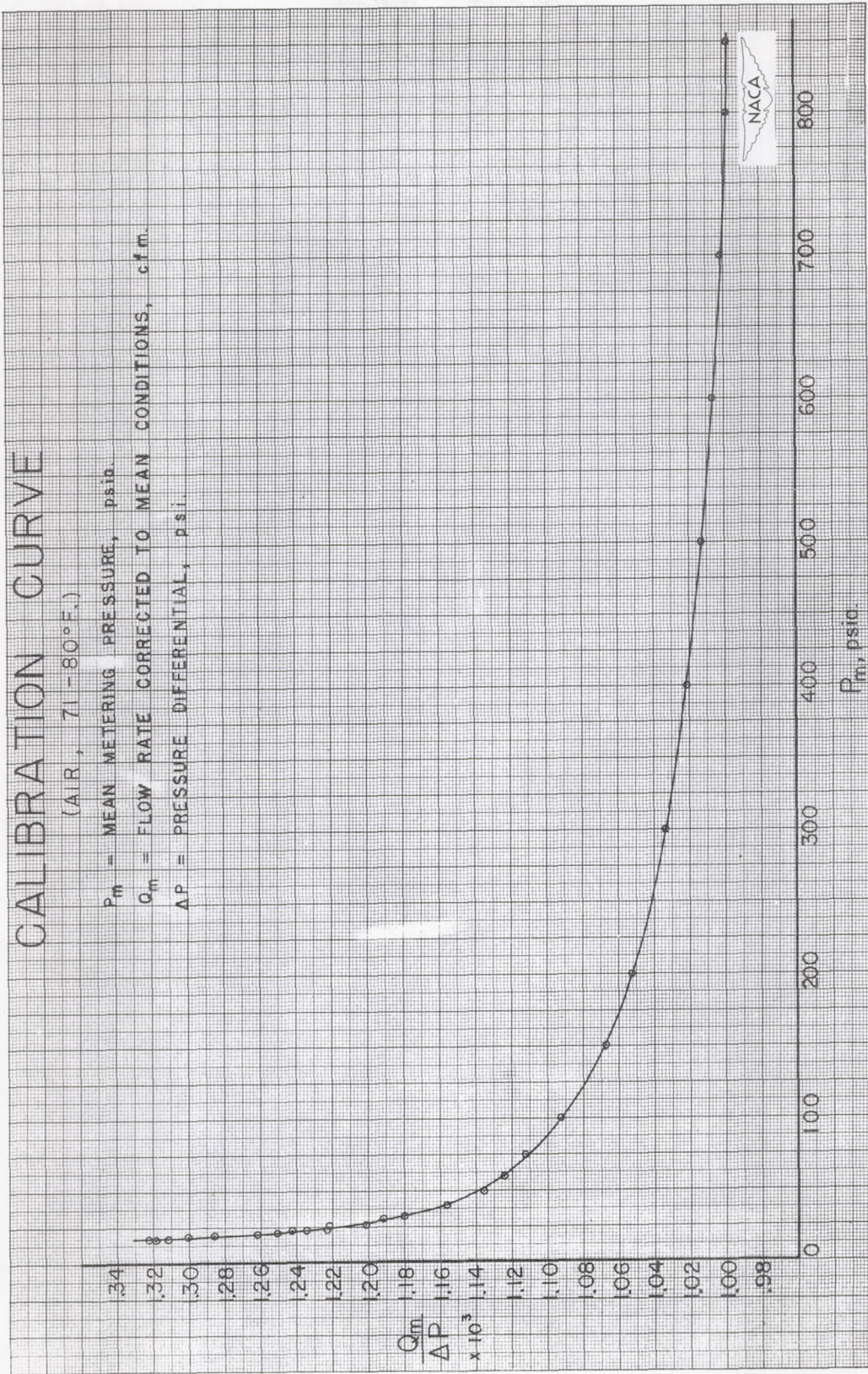


Figure 14.- Calibration curve for air from 71° to 80° F.

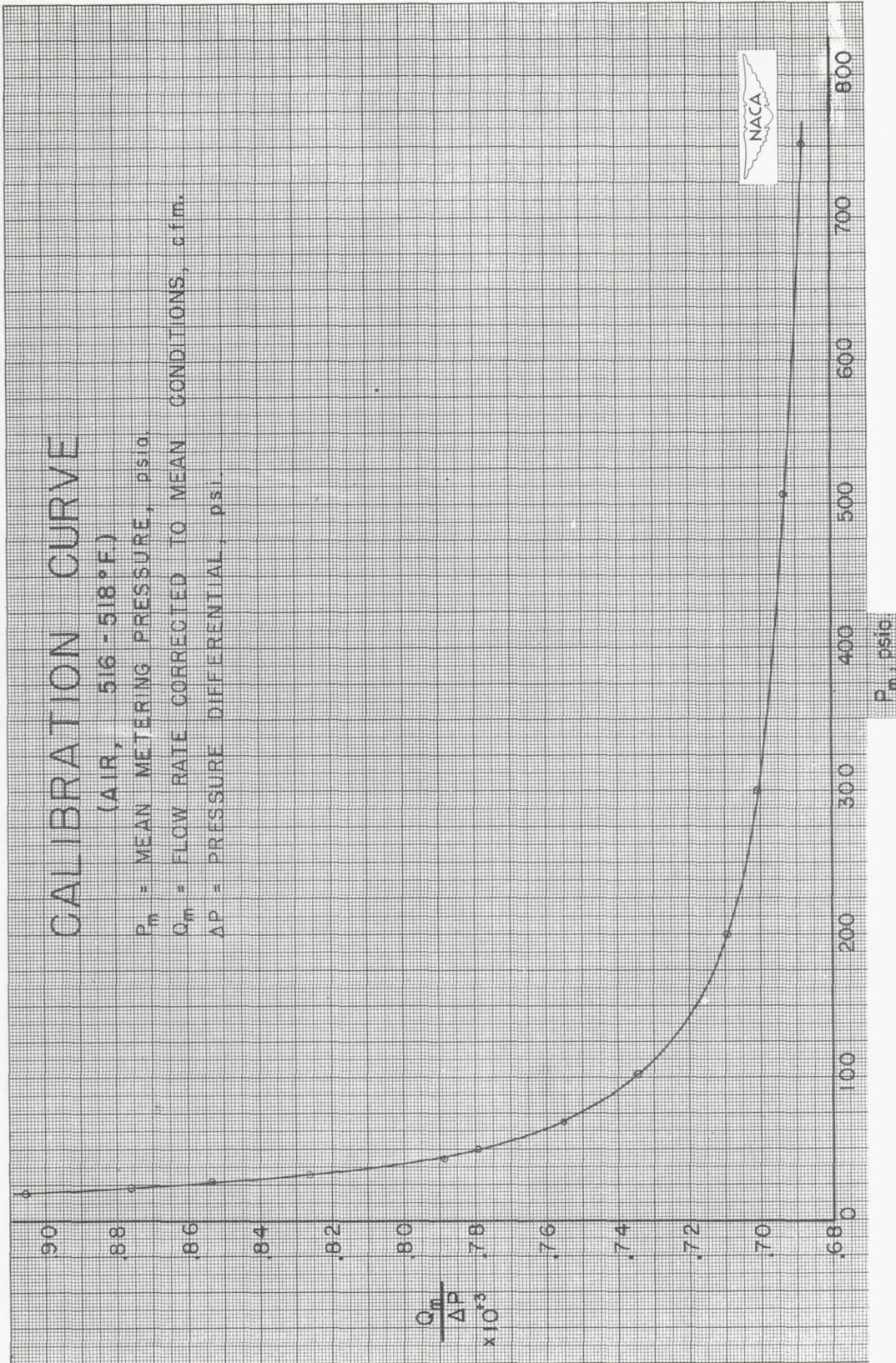


Figure 15.- Calibration curve for air from 516° to 518° F.

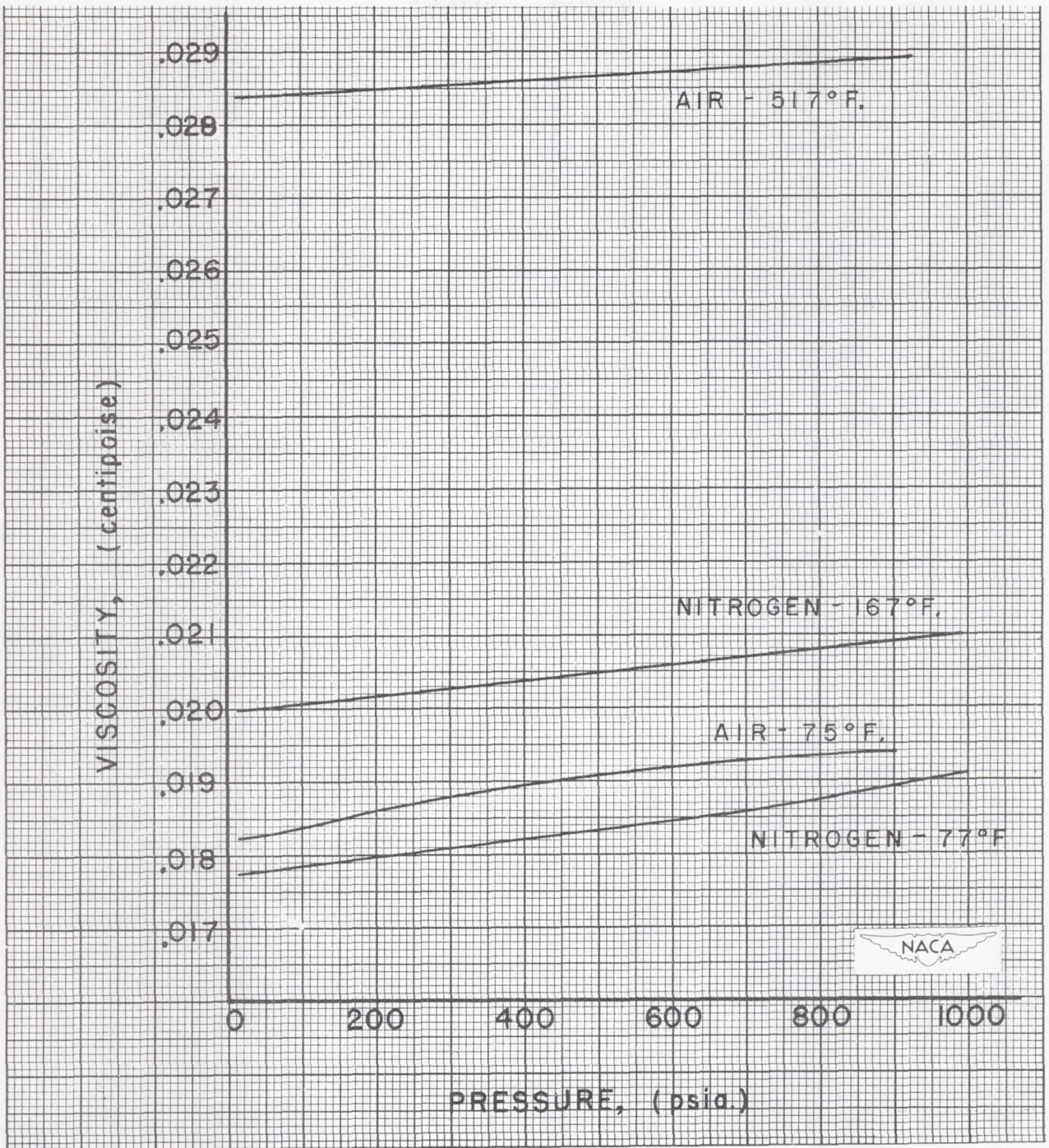


Figure 16.- Viscosity of air. Data for nitrogen from Michels and Gibson (reference 8) shown for comparison.

